OPEN ACCESS Freely available online

PLoS GENETICS

A Bow-Tie Genetic Architecture for Morphogenesis Suggested by a Genome-Wide RNAi Screen in *Caenorhabditis elegans*

Matthew D. Nelson, Elinor Zhou, Karin Kiontke, Hélène Fradin, Grayson Maldonado, Daniel Martin, Khushbu Shah, David H. A. Fitch*

Department of Biology, New York University, New York, New York, United States of America

Abstract

During animal development, cellular morphogenesis plays a fundamental role in determining the shape and function of tissues and organs. Identifying the components that regulate and drive morphogenesis is thus a major goal of developmental biology. The four-celled tip of the *Caenorhabditis elegans* male tail is a simple but powerful model for studying the mechanism of morphogenesis and its spatiotemporal regulation. Here, through a genome-wide post-embryonic RNAi-feeding screen, we identified 212 components that regulate or participate in male tail tip morphogenesis. We constructed a working hypothesis for a gene regulatory network of tail tip morphogenesis. We found regulatory roles for the posterior Hox genes *nob-1* and *php-3*, the TGF-β pathway, nuclear hormone receptors (e.g. *nhr-25*), the heterochronic gene *blmp-1*, and the GATA transcription factors *egl-18* and *elt-6*. The majority of the pathways converge at *dmd-3* and *mab-3*. In addition, *nhr-25* and *dmd-3/mab-3* regulate each others' expression, thus placing these three genes at the center of a complex regulatory network. We also show that *dmd-3* and *mab-3* negatively regulate other signaling pathways and affect downstream cellular processes such as vesicular trafficking (e.g. *arl-1*, *rme-8*) and rearrangement of the cytoskeleton (e.g. *cdc-42*, *nmy-1* and *nmy-2*). Based on these data, we suggest that male tail tip morphogenesis is governed by a gene regulatory network with a bow-tie architecture.

Citation: Nelson MD, Zhou E, Kiontke K, Fradin H, Maldonado G, et al. (2011) A Bow-Tie Genetic Architecture for Morphogenesis Suggested by a Genome-Wide RNAi Screen in *Caenorhabditis elegans*. PLoS Genet 7(3): e1002010. doi:10.1371/journal.pgen.1002010

Editor: Andrew Chisholm, University of California San Diego, United States of America

Received October 8, 2010; **Accepted** January 4, 2011; **Published** March 3, 2011

Funding: This work was supported by NSF grants 0643047 and 0922012 to DHAF. MDN was partially supported by NIH training grant 5T32-HD007520 in Developmental Genetics at NYU. The Caenorhabditis Genetics Center was funded by the NIH National Center for Research Resources. The funders had no role in study design, data collection and analysis, decision to publish, or preparation of the manuscript.

Competing Interests: The authors have declared that no competing interests exist.

* E-mail: david.fitch@nyu.edu

Introduction

Morphogenesis involves the coordinated change in the shape of cells and tissues during development, eventually giving rise to functional structures in the adult animal. Such coordinated change must occur at the correct time and in the proper position. In the case of structures that differ between the sexes, this process must also be regulated sex-specifically. While many genes and pathways are known that regulate development, the identity of genes that link regulation to the execution of morphogenesis have been more difficult to ascertain [1]. The many different cues and signals that must be integrated to control morphogenesis, combined with the complexity of the molecular machinery associated with this process, suggest that a large number of genes and gene products are involved.

To elucidate the molecular mechanisms underlying morphogenesis, the first step is thus to determine what components are involved in its regulation and execution and to determine how they interact in a network. In the pursuit of such an aim, it is advantageous to use a simple model structure that still demonstrates all the properties of cellular morphogenesis. The model we use is the male tail tip of *Caenorhabditis elegans*. This structure is made up of four epithelial ("hypodermal") cells, hyp8–hyp11, which are born during embryogenesis. Embryonic morphogenesis of hyp8–hyp11 leads to the formation of a pointed, whip-like tail tip. The tail tip retains this shape throughout the lifespan of the hermaphrodite. However, during the last larval stage (L4) of males, these conical cells are dramatically remodeled to form the rounded tip of the adult [2–4]. Male tail tip morphogenesis begins when hyp8–11 fuse to form a syncytium; fusion is followed by detachment of the cells from the overlying cuticle. Towards the middle of the L4 stage, the syncytium changes its shape from conical to round and moves anteriorly; these morphogenetic events cease at the end of the L4 stage (Figure 1A). In hermaphrodites, the tail tip cells do not fuse and do not change shape. The tail tip model thus allows the study of a sexual dimorphism at the cellular level. Another advantage of this model is that male-specific mutations in *C. elegans* can be propagated through the self-fertile hermaphrodites, even if the mutations affect male fertility, mating ability, or viability.

A few mutations in genes involved in the regulation of tail tip morphogenesis have been described previously [5–7]. Some of these mutations impede or completely block tail tip morphogenesis, resulting in the retention of the pointed larval tail tip in the adult male, a phenotype that we call "Lep" (Figure 1C). This phenotypic designation is derived from the term "leptoderan,"

Author Summary

Morphogenesis is a process in which cells change their shape and position to give rise to mature structures. Elucidation of the molecular basis of morphogenesis and its regulation would be a major step towards understanding organ formation and functionality. We focus on a powerful model for morphogenesis, the four-celled tail tip of the *C. elegans* male, which undergoes morphogenesis during the last larval stage. To comprehensively determine the components that regulate and execute male tail tip morphogenesis, we performed a genome-wide RNAi screen. We identified 212 genes that encode proteins with roles in fundamental processes like endocytosis, vesicular trafficking, cell–cell communication, and cytoskeletal organization. We determined the interactions among several of these genes to reconstruct a first draft of the genetic network underlying tail tip morphogenesis. The structure of this network is consistent with the "bow-tie architecture" that has been proposed to be universal and confers evolvability and robustness to biological systems. Bow-tie networks have a conserved core which is linked to numerous input and output components. Many components of the network underlying tail tip morphogenesis in *C. elegans* are conserved all the way to humans. Thus, understanding tail tip morphogenesis will inform us about morphogenesis in other organisms.

which—in the taxonomic literature—describes the unretracted, pointed male tail tip in some nematodes related to *C. elegans* [8,9]. Other mutations cause precocious onset of (and thus an extended total period for) tail tip retraction, which results in over-retracted ("Ore") and thus abnormally shortened adult male tails [6] (Figure 1C). Studies of these mutants have revealed a few of the important regulatory components for tail tip morphogenesis. DMD-3 was suggested to be a central regulator of tail tip morphogenesis, as it is required for tail tip retraction in males and is sufficient for inducing ectopic morphogenesis in hermaphrodite tail tips [7]. The gene encoding this DM-domain transcription factor, *dmd-3*, is a homolog of *dmrt1* in vertebrates and *doublesex* in *Drosophila* [10,11]. DMD-3 functions cooperatively and partially redundantly with a closely related factor, MAB-3 [7], also involved in somatic sex determination [12]. TRA-1, the most downstream global regulator in the sex-determination pathway, inhibits the expression of these genes in hermaphrodites [7,13,14]. The initiation of *dmd-3* expression at the proper developmental stage is controlled by the "heterochronic" pathway [7]. Finally, maintenance of *dmd-3* expression levels is regulated by Wnt signaling and a feedback loop involving both MAB-3 and DMD-3 [7].

Only one effector of a cellular process is known to be downstream of DMD-3 and MAB-3, namely the fusogen-encoding gene *eff-1*, which is important for the many fusions that occur between epithelial cells in *C. elegans* [15,16]. DMD-3 and MAB-3 induce expression of *eff-1* through an unknown post-transcriptional mechanism [7].

To find additional genes with roles in tail tip morphogenesis, we carried out a genome-wide, post-embryonic RNAi-feeding screen. This screen identified 212 candidates. Starting with these candidates, we used network model-building [17], transgenic reporter lines and expression epistasis analysis to construct a first draft of the gene regulatory network for tail tip morphogenesis. We found that *dmd-3* expression is regulated by a nuclear hormone receptor (NHR-25), a new heterochronic gene, Hox anteroposterior patterning factors, and GATA transcription factors. NHR-25 is in turn negatively regulated by *dmd-3* and *mab-3*. In addition, *dmd-3* and *mab-3* negatively regulate other signaling modules, including the TGF-β pathway. We also found that DMD-3 and MAB-3 regulate the localization or expression of genes involved in vesicular trafficking/endocytosis, cell polarity and cytoskeletal organization. Our data thus strongly support the hypothesis that DMD-3, MAB-3 and NHR-25 are central regulators of tail tip morphogenesis.

The genetic architecture for tail tip morphogenesis which emerges from this analysis closely resembles the "bow-tie" architecture, a possibly universal characteristic of robust, evolvable systems [18]. A bow-tie network has many inputs and outputs that are connected through a conserved core. Versatile weak linkages form the interface between the core and the input and output. In such a network, there is not a simple flow of information from input to output through the core; instead, there is extensive global and local feedback regulation found at every level [19].

A bow-tie architecture has been found to underlie a variety of biological networks: metabolic networks [20,21], the Toll-like receptor signaling network [22], the epidermal growth factor receptor signaling network [23], the osmolarity glycerol signal-transduction pathway in yeast [24], stress response networks [25] and the immune system [26,27]. In fact, it has been proposed that the bow-tie architecture of regulatory networks is ubiquitous because this structure ensures not only robustness but also evolvability [18,19].

We found evidence for the existence of each aspect of a bow-tie architecture in the gene network governing tail tip morphogenesis. To our knowledge, this is the first time that this kind of network architecture has been explicitly identified in the context of development and morphogenesis. However, we believe that other developing systems are also governed by bow-tie genetic networks, supporting the proposition that this network architecture is universal.

Results

Genome-wide RNAi screen identifies 212 candidate genes involved in male tail tip morphogenesis

To identify tail tip morphogenesis genes, we cultured animals on dsRNA-expressing bacteria from L1 to adult and looked for evidence of defective morphogenesis. Using the Ahringer RNAi-feeding library [28], we screened 16,131 genes, approximately 83% of the genome. Genes that gave a positive Lep or Ore phenotype were screened again; only repeatable positives were kept as candidates. We identified 212 genes, of which 190 produced Lep phenotypes, 14 produced Ore phenotypes, and 8 produced both Lep and Ore phenotypes in a single experiment (Figure 1D). Positives in each category were analyzed for GO-attribute enrichment using FuncAssociate [29]. Relative to the genome, Lep positives showed enrichment of GO-attributes associated with components or processes involved in morphogenesis, such as anchoring junctions and cell migration. However, Ore and Ore/Lep positives were enriched for genes involved in cell division/cytokinesis, and nuclear/chromosome organization (Figure 1D). The 212 candidates are listed and categorized by developmental pathway or annotated cellular process (if known) in Table S1. Raw RNAi data are publicly available along with representative images via the "Male Tail Tip Database" (MTTdb, at http://wormtails.bio.nyu.edu).

We identified components of conserved and widely studied developmental regulatory pathways (e.g. Hox anteroposterior patterning factors, TGF-β signaling module, heterochronic pathway, and GATA transcription factors). Importantly, the screen also identified components of fundamental cellular structures and processes that are likely to be important for the

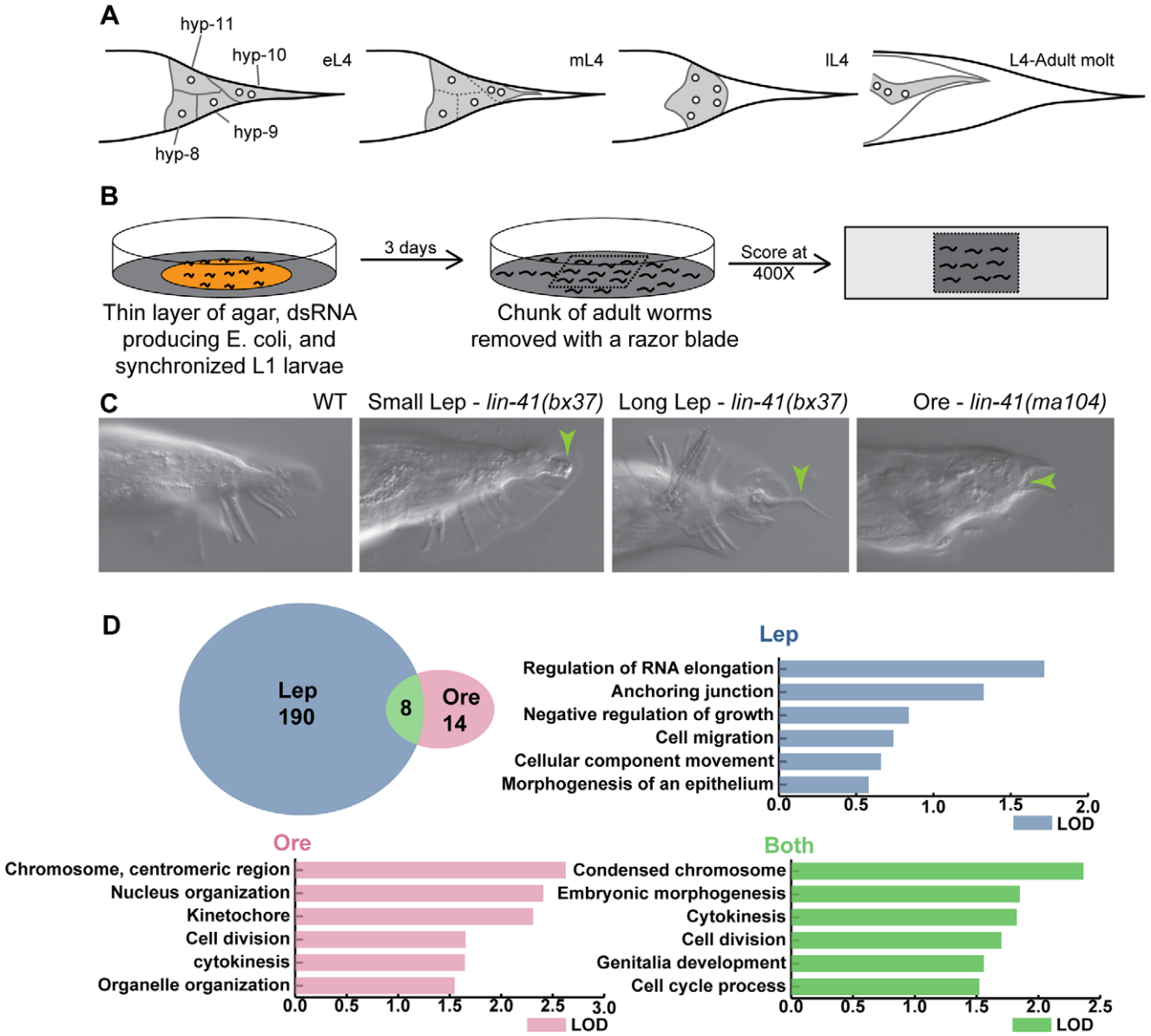

Figure 1. Overview of tail tip morphogenesis and the experimental design for the genome-wide RNAi screen for tail tip defects in male *C. elegans*. (A) Schematic of tail tip morphogenesis: the tail tip cells hyp8–hyp11 fuse and then detach from the overlying cuticle. The newly formed syncytium changes shape—becoming rounded—and migrates anteriorly. By the adult stage, the male tail has flattened out ventrally. (B) Screening methodology: L1 larvae were fed dsRNA-producing bacteria on thin films of nutrient agar and grown to adulthood. A square of agar containing worms was mounted on a slide and scored at 400× magnification. (C) The phenotypes scored included WT (wild type), Lep (leptoderan), and Ore (over-retracted). Additional phenotypes scored but not reported here were spicule morphology and general male tail defects (see http://wormtails.bio.nyu.edu). (D) Distribution of the phenotypes among the 212 positive genes; for 8 genes, Lep and Ore tails were observed in the same experiment. GO attribute enrichment via FuncAssociate [29] for genes causing Lep, Ore and Lep+Ore phenotypes upon RNAi. For each phenotype, the top six categories that were over-represented are indicated with bar graphs depicting the LOD scores, i.e. the log of the odds that the frequency of a GO category is no different than that for all genes in the genome.
doi:10.1371/journal.pgen.1002010.g001

execution of morphogenesis. These include vesicular trafficking/endocytosis, cellular polarity, cytoskeleton, cell junctions, and nuclear export/import. Genes with the most severe and/or most penetrant RNAi phenotypes were selected for further study (Table 1).

Regulatory modules

Hox genes play central roles in shaping animal body plans by distinguishing different fields of cells along the anteroposterior axis [30]. Hox proteins regulate not only the expression of other transcription factors, but also of genes involved in specific processes such as morphogenesis [31]. Our screen has shown that posterior Hox patterning is crucial for tail tip morphogenesis. RNAi knockdowns of the Abd-B homologs *php-3* and *nob-1* postembryonically cause Lep phenotypes (Figure S1A, Tables S1 and S2). Likewise, a *php-3* null allele, *ok919*, results in a 100%-penetrant Lep phenotype of moderate severity (Figure S1B, Table S2). The severity of the *php-3(ok919)* phenotype is increased with *nob-1* RNAi treatment (Table S2). A *nob-1::gfp* translational fusion construct (containing a genomic fragment with the *nob-1* gene and

Table 1. Genes identified in the RNAi screen that caused the most severe and/or penetrant tail tip morphogenesis defects.

Gene	Sequence name	Gene function/domain	Closest human ortholog?	RNAi phenotype[1]	Mutant alleles[2]
abcx-1	C56E6.1	ABC-transporter	ABCG5	Lep	- [3]
arl-1	F54C9.10	ADP-Ribosylation Factor	ARL1	Lep	- [3]
blmp-1	F25D7.3	Zinc finger and SET domain containing protein	BLIMP1	Ore & Lep	*tm548*
bub-1	R06C7.8	Serine/threonine kinase	BUB1	Ore & Lep	- [3]
cdc-42	R07G3.1	Rho-GTPase	CDC42	Lep	- [3]
cdt-1 [7]	Y54E10A.15	DNA-replication licensing factor	CDT1	Ore & Lep	- [3]
daf-4	C05D2.1	TGF-β Receptor	ACVR2B	Lep	- [3]
egl-18	F55A8.1	GATA Transcription factor	GATA1	Lep	*ok290*
inx-12	ZK770.3	Innexin	- [4]	Lep	- [3]
inx-13	Y8G1A.2	Innexin	- [4]	Lep	- [3]
mix-1	M106.1	Chromosome condensation complex, condensin	SMC2	Ore	- [3]
nhr-25	F11C1.6	Nuclear hormone receptor	NR5A2	Lep	*ku217*
nmy-2	F20G4.3	Non-muscle myosin	MYH11	Lep	- [3]
nob-1	Y75B8A.2	Abd-B Homeodomain transcription factor	HOXD12	Lep	- [3]
npp-3	K12D12.2	Nucleoporin	NUP205	Ore	- [3]
npp-6 [7]	F56A3.3	Nucleoporin	NUP160	Ore	- [3]
php-3	Y75B8A.1	Abd-B Homeodomain transcription factor	HOXA11	Lep	*ok919*
plk-1	C14B9.4	polo-like serine/threonine kinase	PLK1	Ore & Lep	- [3]
pri-2 [7]	W02D9.1	Eukaryotic-type DNA primase	PRIM2A	Ore	- [3]
ptl-1	F42G9.9	Tau-like microtubule binding protein	MAP2;MAP4	Lep	*ok621*
ran-3	C26D10.1	Nuclear export/import, RCC1 domain	HERC2;RCC1	Ore	- [3]
rcn-1	F54E7.7	Calcipressin, negative regulator of calcineurin	RCAN1/DSCR1	Lep	*tm2021* [5]
rme-8	F18C12.2	Receptor-mediated endocytosis-defective	DNAJC13	Lep	*b1023*
rpa-1	F18A1.5	DNA-binding replication protein	RPA1	Ore	- [3]
sma-3	R13F6.9	SMAD	SMAD5	Lep	*e491*
smc-4	F35G12.8	Chromosome condensation complex, condensin	SMC4	Ore & Lep	- [3]
wht-5	F19B6.4	ABC-transporter	ABCG1	Lep	*ok806* [6]
xpo-2	Y48G1A.5	Nuclear export factor	CSE1L	Ore & Lep	- [3]

The CGC (Caenorhabditis Genetics Center) gene name, the cosmid-based "GenePairs" name, a brief description and/or predicted human ortholog, and the tail tip phenotype produced by RNAi via feeding are provided for each gene. For some genes, mutants were analyzed and the phenotypes observed in the screen were validated.

[1]For phenotypes see text.

[2]Tested mutant alleles that show tail tip phenotypes similar to the RNAi phenotype (see Table S2 for details).

[3]Not tested or the mutant was not available.

[4]INX-12 and INX-13 are innexins, invertebrate-specific gap junction proteins, apparently unrelated to vertebrate connexins.

[5]Mutants were not crossed to the *him-5(-)* background and thus Lep phenotypes were not quantified. However, a few males (N = 2) were observed with tail tip, ray, and spicule defects.

[6]Mutants did not show Lep phenotypes but did display more widespread male tail defects (i.e. truncated posteriors, missing rays and fan).

[7]Identified as a *let-7* suppressor by Ding et al. (2008) [44].

doi:10.1371/journal.pgen.1002010.t001

9 Kb of the 5′-regulatory region) is expressed in the tail tip cells hyp8–11 throughout larval development in both sexes (Figure 2A and data not shown). A *php-3::gfp* translational fusion driven only by the short 500-bp intergenic region between *nob-1* and *php*-3 shows variable expression in the nuclei of hyp8–11 during tail tip morphogenesis (data not shown). This latter transgene only partially rescues the tail tip phenotypes of *php-3* mutants (Table S2), suggesting that regulatory elements upstream of both *php-3* and *nob-1* are required for appropriate expression of *php-3*. Using a tail tip-specific promoter (from the gene *lin-44* [32]), we observed that expression of the PHP-3::GFP fusion protein product in hyp8–11 is sufficient to rescue the *php-3(ok919)* Lep phenotype (Figure S2A and Table S2). Mosaic animals that only express PHP-3::GFP in a subset of tail tip cells do not show rescue (Figure S2B). These data suggest that Hox-mediated patterning by PHP-3 and NOB-1 is carried out cell-autonomously and is required in all tail tip cells (hyp8–11) for proper morphogenesis.

GATA transcription factors play important regulatory roles during the differentiation of multiple cell types in normal development [33,34] and during tumorigenesis [35]. RNAi knockdown of the gene for the GATA factor *egl-18* resulted in Lep phenotypes (Figure S1C, Tables S1 and S2). An *egl-18* null allele, *ok290*, causes Lep phenotypes of varying severity with 45% penetrance (Figure S1D, Table S2). Another GATA transcription factor that was missed in our RNAi screen, *elt-6*, shares an operon with *egl-18* [36]. We repeated the RNAi treatment against *elt-6* and observed low-penetrance, low-severity tail tip defects (Table S2). RNAi treatment for *elt-6* in the *egl-18(ok290)* mutant strain,

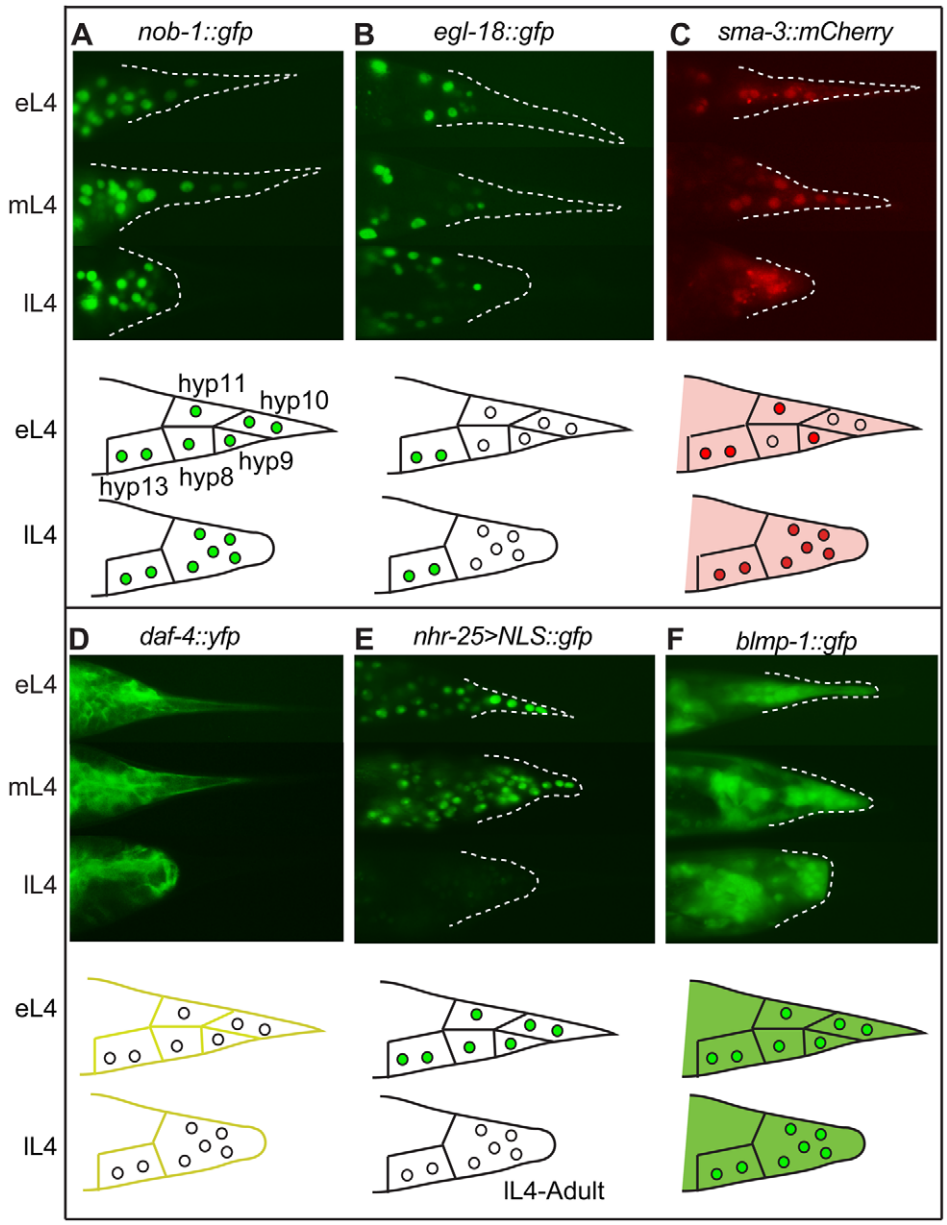

Figure 2. Expression patterns of sample regulatory genes identified in the RNAi screen. Fluorescent micrographs for early, middle and late L4 larvae and schematic drawings for early and late L4 larvae are shown in the upper and lower portions of each panel, respectively. (A) NOB-1::GFP is expressed in hyp8–11 throughout larval development. (B) EGL-18::GFP is expressed in the male tail but not in hyp8–11. (C) SMA-3::mCherry is cytoplasmic in early L4 and begins to accumulate in the nuclei of the tail tip cells. It then remains nuclear and cytoplasmic throughout tail tip morphogenesis. (D) DAF-4::YFP localizes to the membranes of hyp8–11 prior to and during morphogenesis. (E) An *nhr-25* transcriptional reporter shows expression in hyp8–11 at the beginning of morphogenesis, followed by a rapid shutoff. (F) BLMP-1::GFP is expressed in the cytoplasm and nuclei of hyp8–11 throughout larval development.
doi:10.1371/journal.pgen.1002010.g002

however, dramatically increased the penetrance and severity of the tail tip defects, such that tail tip morphogenesis failed altogether in some individuals (Table S2). Interestingly, an *egl-18::gfp* translational fusion is expressed in the nuclei of the main body epidermal syncytium hyp7, but appears to be excluded from the tail tip cells hyp8–11 (Figure 2B). This observation suggests that EGL-18 and ELT-6 function in cells adjacent to the tail tip to regulate tail tip morphogenesis cell-nonautonomously. Furthermore, transforming wild-type animals with the *egl-18/elt-6* operon regulated by the *lin-44* promoter disrupted morphogenesis (data not shown), suggesting that morphogenesis requires exclusion of these GATA factors from hyp8–11. In other epidermal cells, it has been observed that EGL-18 and ELT-6 repress cell fusion [37]. Thus, their exclusion from the tail tip cells may be required to allow tail tip cell fusion and subsequent morphogenesis.

TGF-β signaling is a major conserved cell-signaling module which regulates multiple processes during the development of all animals and also during the progression of cancer [38]. The screen identified two components of this pathway. RNAi treatment against *sma-3*, which encodes a Smad protein, and *daf-4*, encoding the TGF-β receptor, resulted in Lep phenotypes (Figure S1E, Tables S1 and S2). A *sma-3* null allele, *e491*, resulted in a 57%-

penetrant low-severity Lep phenotype (Figure S1F, Table S2). Of the other known components of the TGF-β pathway, only *sma-2* showed any RNAi phenotype: RNAi against *sma-2* significantly enhanced the penetrance of the Lep phenotype of *sma-3(e491)* (Table S2). A transgenic strain expressing a *sma-3::mCherry* translational reporter shows expression at low levels in the cytoplasm of the tail tip of both sexes at the beginning of the L4 stage. In males, the SMA-3::mCherry fusion protein enters the nuclei of hyp8–11 prior to tail tip morphogenesis and remains in both the cytoplasm and nuclei during morphogenesis (Figure 2C). In hermaphrodites, SMA-3::mCherry remains cytoplasmic throughout L4 and never enters the nuclei (data not shown). The dynamic localization pattern of SMA-3::mCherry suggests that TGF-β-mediated gene expression occurs concurrently with tail tip morphogenesis. Consistent with this hypothesis, DAF-4::YFP fusion protein localizes to the plasma membranes of hyp8–11 during tail tip morphogenesis (Figure 2D). Taken together, the RNAi results, loss-of-function mutant phenotypes and expression patterns of *sma-3* and *daf-4* suggest that TGF-β signaling is required during tail tip morphogenesis.

Previous work has shown that Wnt signaling plays a crucial role in the regulation of tail tip morphogenesis [5]. Consistent with those findings, the RNAi screen identified additional genes that are in or interact with the Wnt pathway. RNAi treatments against *sys-1* (β-catenin) and *lit-1* (Nemo-like kinase) each resulted in Lep phenotypes (Table S1, Figure S3C, S3D). A transgenic strain expressing a SYS-1::GFP fusion protein shows faint cytoplasmic expression in hyp8 and hyp11 but not in hyp9 or hyp10 (Figure S3C). A strain expressing a LIT-1::GFP fusion protein shows nuclear expression in hyp9 and hyp10 but not in hyp8 or hyp11 prior to morphogenesis (Figure S3D).

We identified multiple nuclear hormone receptor genes in our screen: *nhr-9*, *nhr-23*, *nhr-25* and *nhr-165*. NHR-25 is the *C. elegans* homolog of FTZ-F1 [39] which is a highly conserved protein with diverse functions regulating embryonic patterning [40,41], and ecdysone-mediated molting in *Drosophila* [42]. Both *nhr-25* RNAi and a hypomorphic allele, *ku217*, showed Lep phenotypes (Figure S1G and S1H, Tables S1 and S2). Furthermore, *nhr-25* RNAi treatments on the *ku217* strain showed a complete lack of male tail morphogenesis in 33% of the animals ($N = 24$, Table S2), a phenotype reminiscent of the *mab-3(e1240);dmd-3(ok1327)* double mutant [7]. We were not able to produce transgenic lines expressing NHR-25 fusion proteins due to lethality, as previously reported [43]. Instead, we made a transgenic strain expressing a transcriptional reporter containing the 5′- and 3′-regulatory regions for *nhr-25*. This reporter shows a dynamic expression pattern in which expression in hyp8–11 is intense prior to and at the beginning of morphogenesis, rapidly shuts off in late L4, and is never on in adult animals ($N = 34$ adults) (Figure 2E). RNAi against another nuclear hormone receptor gene, *nhr-165*, showed a low-penetrant, mild, yet reproducible Lep phenotype upon RNAi treatment (Table S1, and Figure S3A). An *nhr-165::gfp* translational reporter shows nuclear expression in the lateral hypodermis (hyp7, but not hyp8–11) near the time of larval molts. This expression is highest and seen in the largest number of cells in the tail prior to the L3–L4 molt (Figure S3A).

New genes that temporally control morphogenesis

The heterochronic pathway ensures that tail tip morphogenesis is initiated precisely at the beginning of the L4 stage [6]. We identified genes in this pathway: the zinc-finger transcription factor gene *blmp-1*, and known suppressors of the miRNA *let-7* [44]. BLIMP-1 is a transcriptional repressor that regulates ecdysone-mediated molts in *Drosophila* [45] and differentiation of multiple cell types in humans and mice, such as lymphocytes [46] and primordial germ cells [47,48]. Intriguingly, BLIMP-1 is a target of *let-7*-mediated degradation in Reed-Sternberg cells, a Hodgkin-lymphoma cell line, suggesting a possibly conserved interaction with the heterochronic pathway, of which *let-7* is a member [49,50]. RNAi treatments directed against *blmp-1* produced Ore phenotypes (Table S1). A deletion allele, *tm548*, produces an Ore phenotype with 100% penetrance (Table S2) due to precocious initiation of tail tip morphogenesis during the L3 stage ($N = 26$, data not shown). A transgenic line expressing a BLMP-1::GFP fusion protein shows both nuclear and cytoplasmic expression in hyp8–11 throughout development, although cytoplasmic expression is most intense during tail tip retraction (Figure 2F).

Of the 41 suppressors of *let-7* lethality identified by Ding et al. [44], six were positives in our screen. RNAi knockdown of two (*pri-2*, *npp-6*) resulted in the Ore phenotype, of two others (*spg-7*, *smo-1*) in the Lep phenotype and of two further genes (*cdt-1*, *xpo-2*) in both phenotypes in a single experiment. Four of these genes—*pri-2*, *npp-6*, *cdt-1*, and *xpo-2*—are predicted by N-Browse [17] to interact in a subnetwork that includes other genes for which RNAi knockdown also produced Ore phenotypes (Figure 3). It is thus possible that these additional genes also influence the timing of tail tip morphogenesis. It is still unclear why both Ore and Lep phenotypes are observed in a single experiment. One possible explanation is that precision in timing of tail tip morphogenesis is lost when certain gene-products are removed. In this case, morphogenesis might begin too early in one animal and too late in another, leading to Ore tails and Lep tails, respectively.

Post-transcriptional regulation is important for tail tip morphogenesis

Post-transcriptional regulation appears to play an important role during the coordination of tail tip morphogenesis, as our screen has identified multiple genes that encode RNA splicing factors, kinases, phosphatases and ubiquitinating enzymes. One such gene is *ubc-12*, which is a part of the NED-8 conjugating system and has been shown to be important in epidermal differentiation during embryogenesis in *C. elegans* [51]. RNAi-knockdown of *ubc-12* resulted in larval lethality in the RNAi hyper-sensitive *rrf-3(-)* background (Table S4). However, we identified *ubc-12* in a pilot screen which was carried out in the wild-type background; *ubc-12* RNAi treatments produced a highly penetrant and severe tail tip defect (Figure S3B). UBC-12::GFP expresses intensely in the cytoplasm of hyp10 just prior to and during tail tip retraction (Figure S3B).

Components of junctions, organelles, and the cytoskeleton required for tail tip morphogenesis

We identified many genes known to play central roles during the execution of morphogenesis. Such genes encode proteins involved in vesicular trafficking, endocytosis, cell-cell communication, cytoskeletal rearrangement, establishment of cellular polarity and cell-cell transport.

Vesicular trafficking/endocytosis machinery. Several genes identified in our screen are predicted to function in endocytosis or vesicular trafficking, including *arl-1*, *agef-1*, *rme-8*, *rab-6.2*, *dab-1* and *rab-14*. We focused our attention on *rme-8* and *arl-1* because of their strong RNAi phenotypes. RNAi-knockdown of *rme-8*, a gene essential for receptor-mediated endocytosis [52], produces a dramatic disruption in tail tip retraction and male tail morphogenesis in general. Adult males lack rays and a fan and the tail tip is completely unretracted; however, spicules are present (Figure 4A). The same phenotype was seen in the temperature-sensitive lethal allele, *rme-8(b1023*ts*)*, at the permissive temperature

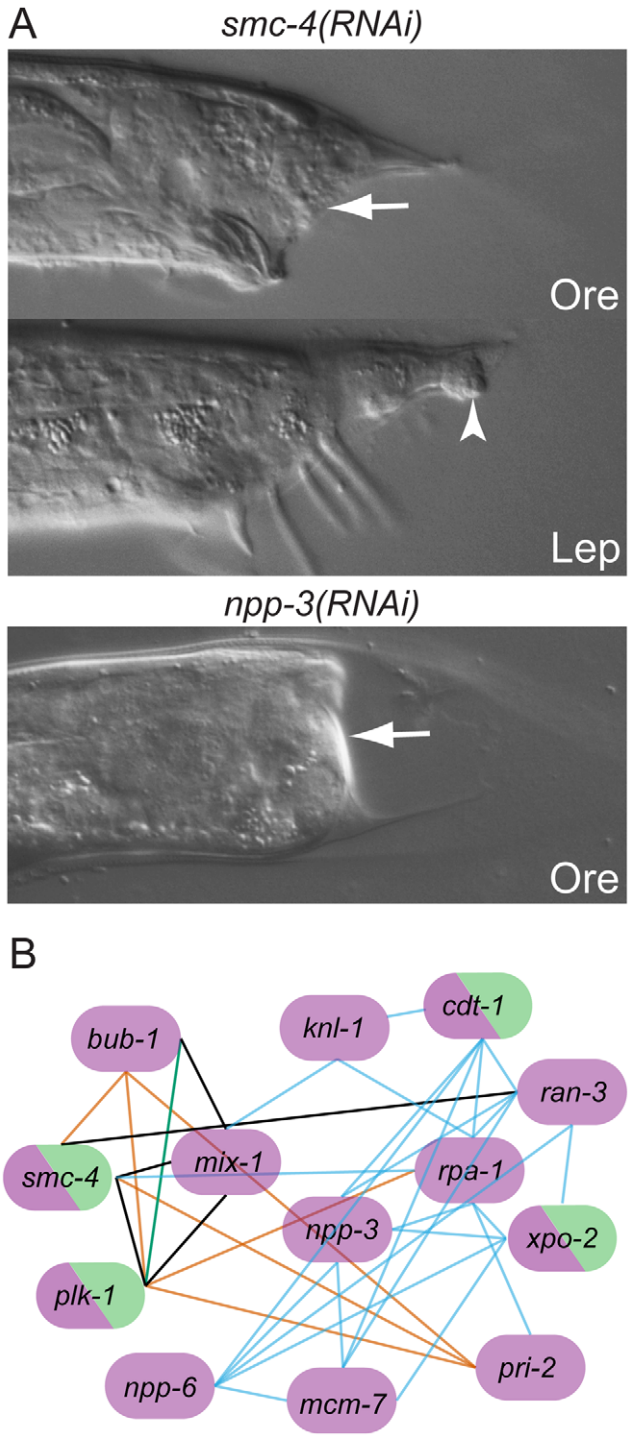

Figure 3. Genes with Ore-like phenotypes. (A) DIC images of male tails: RNAi of *smc-4* resulted in Ore (arrow) and Lep (arrowhead) phenotypes. *npp-3* RNAi resulted in severe Ore tails (arrow). (B) Subnetwork of genes that produce the Ore phenotype as reconstructed by N-Browse [17]. Thirteen of the 22 genes with an Ore phenotype are tightly clustered: purple, Ore RNAi phenotype; green, Lep RNAi phenotype; black edges: predicted genetic interactions; orange edges: expression correlation; blue edges: phenotypic correlation in the embryo; green edges: protein-protein interaction (multiple data sources, see [17]).
doi:10.1371/journal.pgen.1002010.g003

(Table S2). RME-8::GFP is localized in small round structures (which we interpret as vesicles) that form at the apical surfaces of the detaching tail tip cells and are concentrated at the cell surfaces during retraction (observed in 50/52 cases) (Figure 4A). Tail tip retraction is also disrupted upon knocking down *arl-1*, encoding an ADP-ribosylation factor-like protein (Figure 4B). Expression of ARL-1::GFP is cytoplasmic and extremely faint in hyp8–11 during early L4, prior to tail tip retraction (28/32 animals) (Figure 4B). Occasionally, bright expression is seen in hyp10 (4/32 animals). ARL-1::GFP becomes more intense and localizes to puncta (possibly vesicles) after rounding of the cells has occurred (Figure 4B). In adult animals, hypodermal expression is absent, but neuronal expression (e.g., in PHCL and PHCR) is apparent in all animals ($N = 35$).

Gap junctions. Transmission electron microscopic reconstruction of the tail tip revealed the presence of gap junctions between the hyp cells in the tail [3]. The gap junction protein-encoding genes, *inx-12* and *inx-13* show Lep phenotypes of varying severity upon RNAi treatment (Figure 4C, 4D and Table S1). Transcriptional reporters for both *inx-12* (YFP) and *inx-13* (CFP) are expressed at a low level in hyp8–11 prior to tail tip morphogenesis but more highly during retraction (Figure 4C, 4D). Because this increase in expression occurs after the tail tip cells have fused with each other, we predict that these innexins establish new junctions between the tail tip syncytium and other cells, although it is also possible that they form hemichannels.

Cell polarity and cytoskeleton. Our data suggest that morphogenesis of the tail tip is carried out by an asymmetric cytoskeletal rearrangement that drives the anteriorly directed "retraction". The RNAi screen identified a role for the Rho-GTPase encoded by *cdc-42*, for non-muscle myosins encoded by *nmy-1* and *nmy-2*, for a Rho-GEF encoded by *ect-2*, for an intermediate filament protein encoded by *ifc-2*, and for a microtubule binding protein encoded by *ptl-1* (Table S1). RNAi-knockdown of *cdc-42* results in a highly penetrant and severe Lep phenotype (Figure 4E, Table S1). A CDC-42::GFP fusion protein is diffusely distributed in the cytoplasm of the tail tip cells at the early L4 stage and then localizes to foci at the apical surfaces of the tail tip cells just before retraction begins at mid-L4 (Figure 4E). During retraction, CDC-42::GFP again becomes diffuse in the cytoplasm. RNAi-knockdown of *nmy-2* also resulted in tail-tip retraction defects (Figure 4F and Table S1). Using confocal microscopy and 3-dimensional reconstruction of L4 males expressing *nmy-2::gfp*, we observed a cap of NMY-2::GFP that forms at the posterior end of the rounding, retracting tail tip (Video S1 and Figure S4) and along the ventral surface where the tail tip cells begin to pull away from the larval cuticle. Also, foci of NMY-2::GFP form at the apical surfaces with fibrous projections from these foci into the cells (Figure S4). Later, NMY-2::GFP becomes very intense in the region where the ray tips will form (Video S2). A strain expressing NMY-2::mCherry shows the same pattern (Figure 4F).

ABC-transporters. ATP-binding cassette (ABC) transporters play central roles in bacterial drug resistance, and mammalian metabolism and immune responses [53]. The *C. elegans* ABC transporter-encoding gene, *abcx-1*, showed a Lep phenotype upon RNAi (Figure 4G and Table S1). An ABCX-1::GFP fusion protein shows male-specific expression during the transition from L3 to L4 both on the membrane and in the cytoplasm in hyp8, 9 and 11, but not in hyp10. This expression fades and becomes extremely faint during tail tip retraction (Figure 4G).

Genes expressed in the PHC neurons

Adjacent to the tail tip cells lie the dendritic projections of the PHC neurons. Two genes that produced Lep phenotypes upon

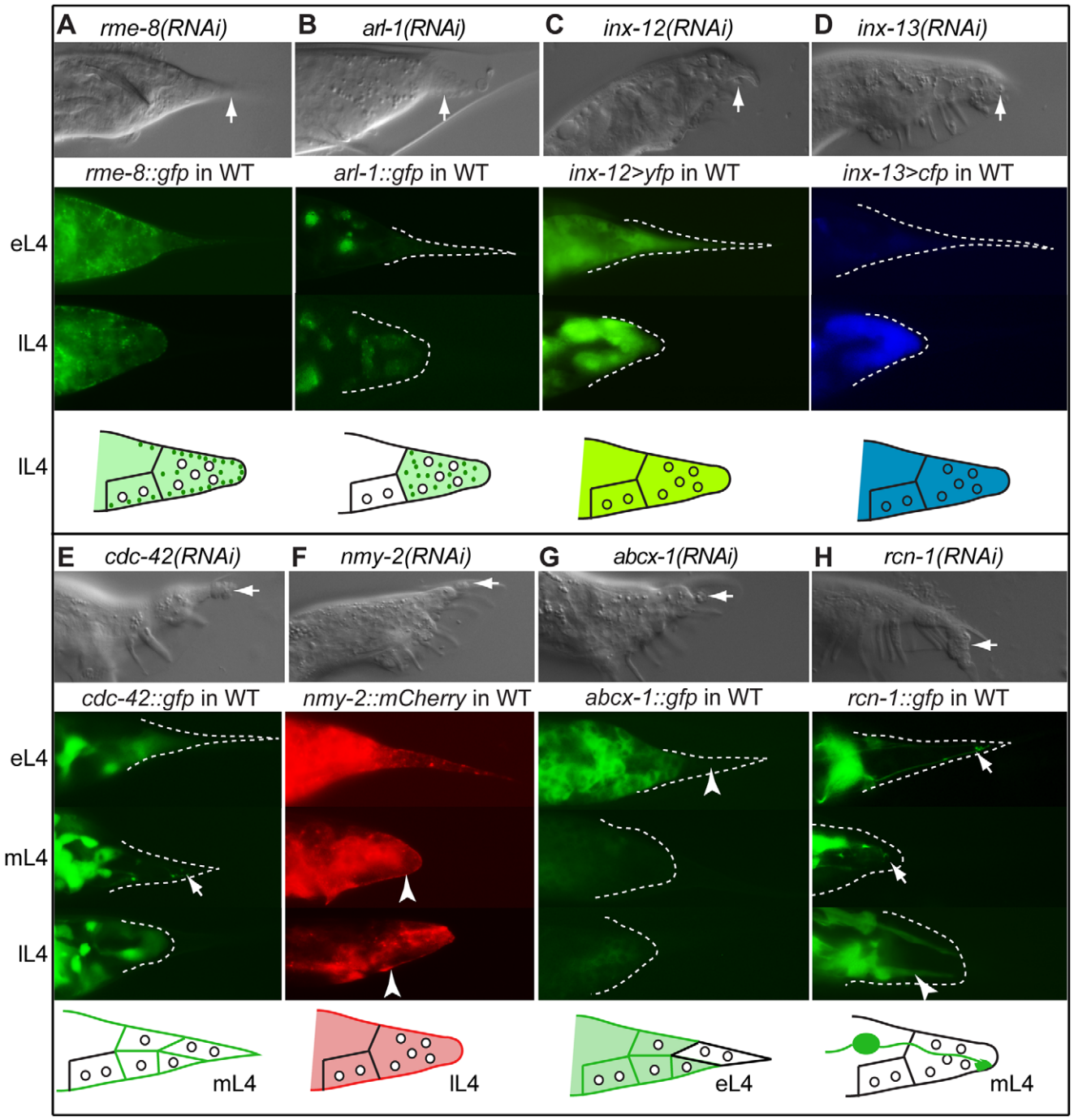

Figure 4. Effectors of morphogenesis identified in the RNAi screen. DIC images of RNAi phenotypes in adult males (top of each panel), expression patterns in the male tail of early L4 (eL4), mid L4 (mL4) and/or late L4 (lL4) (middle of each panel), and schematic of expression/localization patterns (bottom of each panel). Arrows in the DIC images indicate Lep tail tips; arrows in the fluorescent images indicate localization patterns of interest. (A) *rme-8(RNAi)* results in a total failure of tail tip morphogenesis. RME-8::GFP localizes to the edge of detaching and retracting tail tip cells as puncta (depicted as dark green dots in the schematic). (B) *arl-1(RNAi)* causes a disruption of tail tip retraction. ARL-1::GFP is expressed cytoplasmically at extremely low levels in hyp8–11 prior to morphogenesis (eL4); during morphogenesis (lL4), it localizes to distinct puncta (dark green dots in the schematic). (C, D) *inx-12(RNAi)* and *inx-13(RNAi)* result in subtle Lep phenotypes. Reporters for *inx-12* and *inx-13* are expressed in tail tip cells prior to and during morphogenesis. (E) *cdc-42(RNAi)* results in a Lep phenotype. CDC-42::GFP is cytoplasmic prior to tail tip retraction, localizes to the membranes and discrete puncta during retraction (arrow), and becomes cytoplasmic again in late L4 and adults. (F) *nmy-2(RNAi)* results in Lep phenotypes. NMY-2::mCherry localizes to the posterior end of retracting tail tip cells and to the ventral surface of the male tail (arrowheads). (G) *abcx-1(RNAi)* results in Lep phenotypes. ABCX-1::GFP is expressed in hyp8, 9 and 11 prior to but not during morphogenesis. Expression is absent from hyp10 (arrowhead). (H) *rcn-1(RNAi)* causes Lep phenotypes. RCN-1::GFP is expressed in PHCL and PHCR (arrows), as well as in other more anterior neurons during tail tip morphogenesis. After morphogenesis, expression is intense in the phasmid socket cells (arrowhead).
doi:10.1371/journal.pgen.1002010.g004

RNAi treatment are expressed in these neurons but not in the tail tip cells: the calcipressin-encoding gene *rcn-1* [54] and *ptl-1*, a gene encoding a tau-like microtubule-associated protein [55,56]. A null allele of *ptl-1*, *ok621*, produced Lep phenotypes with 23% penetrance (Table S2). PTL-1::GFP and RCN-1::GFP fusion proteins are expressed in the PHC neurons prior to and during hypodermal morphogenesis. In adults, PTL-1::GFP is expressed in most neurons of the tail (data not shown). RCN-1::GFP is expressed in most tail neurons and in the support cells of the phasmid neurons (socket cells, Figure 4H). This pattern is consistent with the previously described adult expression pattern of RCN-1 [54].

A genetic architecture of tail tip morphogenesis

With a list of genes required for tail tip morphogenesis, we next sought to characterize the interactions between these genes. We constructed a working hypothesis for these interactions using N-Browse, a publicly available database which integrates the information from numerous genome-wide studies to build gene networks [17]. We manually entered our candidate genes into N-Browse, excluding those that did not have predicted functions or known interactors. N-Browse produced a genetic network that included not only our candidate tail tip morphogenesis genes, but additional genes predicted to be nearest-neighbor interactors. To the resulting N-Browse network, we manually added gene interactions (edges) based on published work not represented in N-Browse [6,7,44,51,57–61] (Figure 5). This analysis predicts the involvement of genes not identified in our screen. We tested two of these predictions by repeating RNAi knockdown with different methods and/or by scoring larger numbers of males. We could thus validate roles in morphogenesis for *elt-6* and *vav-1*. *elt-6* has genetic interactions with *egl-18* (positive in our screen) in other contexts. It showed a low-penetrance Lep phenotype when the RNAi experiment was repeated and more males were scored. In addition, *elt-6(RNAi)* enhances the Lep phenotype of *egl-18(ok290)* mutants (Table S2). Also, the network model predicts that *vav-1* has interactions with *php-3, cdc-42* and *inx-12* (all positives in our screen, Figure 5). Although *vav-1* treatment by RNAi via feeding did not result in detectable phenotypes, administering RNAi against *vav-1* by soaking did cause tail tip defects (data not shown).

We next asked whether the network model—developed from information in other systems—has biological relevance for tail tip morphogenesis. To this end, we tested a selection of the predicted interactions by genetic and expression epistasis analyses. The results are detailed below.

Components upstream of *dmd-3* and *mab-3*. Previous work [7] proposed that *dmd-3* and *mab-3* play a central role in the regulation of tail tip morphogenesis. If so, we would predict that many regulatory pathways interact with these genes. To test this prediction, we compared *dmd-3* expression in various mutant backgrounds to that in wild-type males. In wild type, the expression of a *dmd-3>yfp* transcriptional reporter coincides with the morphogenesis of the male tail tip, as previously reported [7] (Figure 6A). Expression of *dmd-3>yfp* is reduced in the *php-3(ok919)* mutant background ($N = 32$) and upon treatment with *nob-1* RNAi ($N = 24$) (Figure 6B, 6C). Removing *nob-1* by RNAi in the *php-3(ok919)* background results in a further reduction of *dmd-3>yfp* expression ($N = 26$) (Figure 6D). Removing *egl-18* and *elt-6* results in a reduction of *dmd-3>yfp* expression as well ($N = 16$) (Figure 6E). In each case, *dmd-3>yfp* expression is initiated at the correct time, but the levels of expression are reduced, suggesting that *php-3*, *nob-1*, *egl-18*, and *elt-6* are positive regulators of *dmd-3*, but are not required for initiation of *dmd-3* expression. In the *nhr-25(ku217)* mutant background, *dmd-3>yfp* expression is completely blocked in hyp8–11, while expression in the PHCL/R neurons is not affected ($N = 22$; Figure 6F). Thus, *nhr-25* is required for the initiation of *dmd-3*. In the *blmp-1(tm548)* mutant background, *dmd-3>yfp* is activated precociously in hyp(8,9,11), but is not expressed in hyp10 ($N = 21$) (Figure 6G). We also tested if GATA expression is influenced by Hox expression; however, EGL-18::GFP expression in a *php-3(ok919)* background is the same as in wild type (data not shown).

Negative regulation downstream of *dmd-3* and *mab-3*. Because DMD-3 functions partially redundantly with MAB-3, we examined various transgenic reporters in the *mab-3(e1240);dmd-3(ok1327)* double mutant background. Our *nhr-25* transcriptional reporter is completely shut off during late L4 in wild-type males, but maintained in *mab-3(e1240);dmd-3(ok1327)* double-mutant males (compare Figure 6H and 6I, respectively). Expression persists in hyp8–11 into adulthood ($N = 32$). Since *nhr-25* is required for *dmd-3* expression, this observation suggests that *dmd-3* and/or *mab-3* regulate *nhr-25* via a negative feedback loop.

Negative interactions are also observed between *dmd-3/mab-3* and the TGF-β pathway and between *dmd-3/mab-3* and the *vav* oncogene homolog, *vav-1*. In *mab-3(e1240);dmd-3(ok1327)* males, nuclear SMA-3::CFP remains bright in hyp8–11 into adulthood ($N = 18$) (Figure 6K), whereas such adult expression is never observed in wild-type males (Figure 6J, $N = 31$). Thus, *dmd-3* and/or *mab-3* negatively regulate TGF-β signaling in hyp8–11. A strain expressing a transcriptional reporter for *vav-1* shows bright expression in hyp8–11 prior to and during morphogenesis (Figure 6L). Expression fades in the tail tip during adulthood and is only seen in a small subset of other cells. However, in *mab-3(e1240);dmd-3(ok1327)* males, expression of this reporter persists brightly in the adult tail tip and in a larger subset of cells (Figure 6M). Thus, *dmd-3* and/or *mab-3* negatively regulate *vav-1*, a new interaction not predicted by the N-Browse network model.

Cellular machinery regulated by *dmd-3*. We also wanted to determine how genes involved in executing morphogenesis might be affected by DMD-3 and MAB-3. In the *mab-3(e1240);dmd-3(ok1327)* mutant background, localization of RME-8 is disrupted. RME-8::GFP is still localized to puncta, but it is distributed more evenly in the cytoplasm (in 39/51 males) instead of concentrated near the apical surfaces of the cells (Figure 7A). Thus, *dmd-3* and/or *mab-3* are upstream of RME-8 localization during tail tip morphogenesis. At early L4, ARL-1::GFP is expressed intensely in the hyp10 cell in most *mab-3(e1240);dmd-3(ok1327)* mutant males (21/34 males), whereas this reporter was expressed intensely in only few wild-type males (4/32; Figure 7B). On the other hand, mutant adults lack the PHCL/R expression (absent in 40/41 males) that is present in all wild-type males ($N = 35$) (Figure 7B). Thus, *arl-1* expression is controlled by *dmd-3* and/or *mab-3*, positively in the neurons but negatively in hyp10. Finally, we examined the expression and localization of NMY-2 in *mab-3(e1240);dmd-3(ok1327)*males. DMD-3 and MAB-3 do not appear to affect the expression level of NMY-2::mCherry (Figure 7C). However, we did not observe the accumulation of NMY-2 at the posterior tip where rounding would occur in wild type. This lack of localization is consistent with the fact that the tail tip cells never change their shape in the *mab-3(e1240);dmd-3(ok1327)* mutant strain (Figure 7C). We still observe NMY-2 localization at the positions where the rays would normally form, even though rays do not form in this strain (not shown). This latter NMY-2 localization correlates with a small amount of pulling away ("anterior retraction") from the overlying cuticle in the *mab-3(e1240);dmd-3(ok1327)* mutant males (not shown). Thus, while transcription of *nmy-2* is presumably normal, DMD-3 and MAB-3 partially affect the localization of NMY-2 in the tail tip; this effect is likely to be indirect.

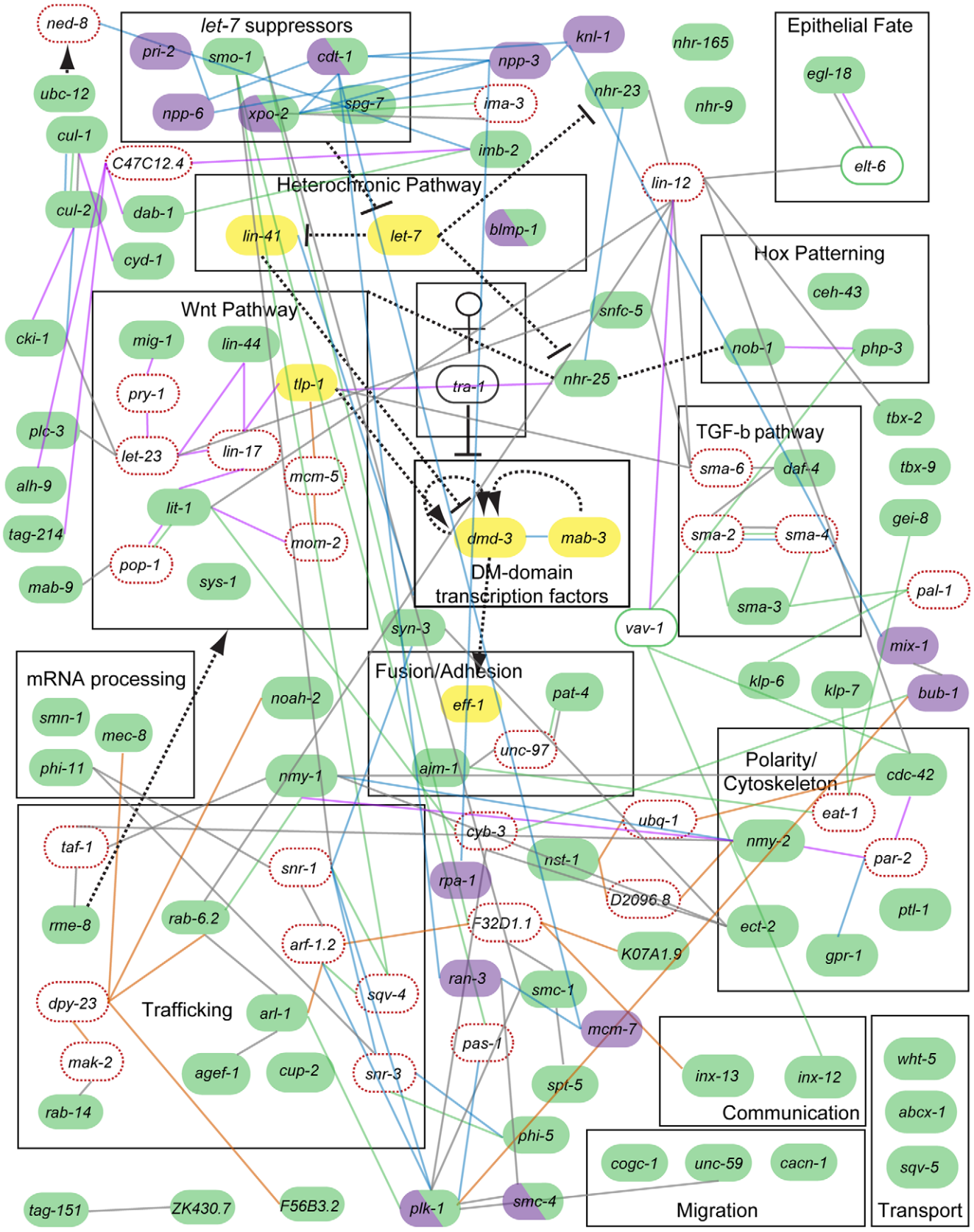

Figure 5. A partial genetic network of tail tip morphogenesis as predicted by N-Browse [17] (thin lines) and other published work (thick dashed lines) [7,44,57–59,61]. Clusters of pathways or functional groups are surrounded by boxes to represent their proximity within the network and/or functional interactions in modules. Nodes (genes): green, Lep positives identified in the screen; purple, Ore positives identified in the screen; green/purple, Lep+Ore positives from the screen; yellow, previously identified tail tip genes; green boundary (unfilled), not identified in the

screen but suggested by the network and experimentally validated; red boundary (unfilled), not positive in the screen and not further tested. Edges (lines) represent the following types of data concerning interactions: dashed black: published and experimentally validated interactions; blue: interologs (conserved interactions between pairs of proteins that have interacting homologs in other organisms); gray: predicted genetic interactions; purple: experimentally verified genetic interactions; green: protein-protein interactions; orange: expression correlations.
doi:10.1371/journal.pgen.1002010.g005

We tested 10 additional gene pairs for epistatic interactions, however, in these experiments, the expression of the reporters in the mutant background did not differ from expression in wild-type males (Table S5). Experimentally validated interactions between genes involved in male tail tip morphogenesis are shown in Figure 8. As will be discussed below, the architecture of this part of the network is consistent with a bow-tie structure, with *dmd-3*, *mab-3* and *nhr-25* at the core and a number of genes in the input and output fans.

Discussion

Genome-wide RNAi screen

Here, we used systemic RNAi to identify components that are involved in male-specific morphogenesis of the tail tip of *C. elegans*. RNAi via feeding in *C. elegans* provides a simple yet powerful means for identifying the regulatory and structural components and pathways of developmental processes [28,62]. The methodology we employed (Materials and Methods and Figure 1B) allowed us to quickly score for subtle defects in morphogenesis at high magnification. Many of the genes we identified have roles in embryonic processes and are lethal when knocked down (e.g. *nob-1, cdc-42*). This justifies our approach to treat worms with RNAi postembryonically and it underscores the power of RNAi as a tool for identifying postembryonic roles of genes that have essential embryonic functions. To minimize the number of false negatives, we performed the screen on the RNAi hypersensitive strain, *rrf-3* [63]. For a number of reasons, however, we believe that there are still other tail tip genes to be identified. First, our screen did not cover the entire genome (approx. 83%). Second, because of complete larval lethality, about 2% of the genes in our screen were not scored, including the known tail tip regulator *lin-41* [6] (Table S4). Third, of the previously known tail tip genes, only *lin-44*, which encodes for the Wnt ligand, was found in the screen. Other known tail tip genes, *tlp-1* and *dmd-3*, which have representative clones in the library, were missed. Finally, two genes (*elt-6* and *vav-1*) not found in the screen, but predicted by the N-Browse network analysis, turned out to have RNAi-induced tail tip phenotypes when treated in a different genetic background (i.e. *elt-6* RNAi in the *egl-18(ok290)* background) or by soaking instead of feeding (*vav-1*). The number of false positives is likely to be very small since only genes which were positive in the primary and secondary screen were considered. The 212 candidate genes identified in this process were significantly enriched with morphogenesis-related GO attributes relative to the genome at large, consistent with what would be predicted if our screen were successful. Some candidates were studied further to elucidate their roles in regulating or effecting tail tip morphogenesis.

Network architecture and features

Developmental decisions, such as the initiation of morphogenesis, require the input of multiple signaling pathways and result in a coordinated response by many different components of the cell. The response must be robust against perturbations from the internal and external environment. Robustness and precision of biological processes are thought to be facilitated by a bow-tie (or hourglass) architecture of the gene regulatory network [18,19]. Characteristics of bow-tie networks include the following. (1) Many inputs and outputs are connected to a conserved core. (2) Versatile weak linkages form the interface between input and core and between core and output. (3) Systems control is facilitated by positive and negative feedback at every level. (4) Modularity and partial redundancy or degeneracy are two other properties of the bow-tie network architecture that contribute to the robustness of biological systems [19,64].

We used the data about gene interactions described here in combination with published information to delineate a first draft of the gene regulatory network underlying tail tip morphogenesis in *C. elegans* males. Although the reconstruction of this network has only just begun, we already find many features that are consistent with bow-tie architecture.

Modularity

A network of interactions is called modular if it can be subdivided into relatively autonomous components (modules) that are built of highly connected parts but are more loosely connected to other modules [65]. Modularity is a major contributor to the robustness and evolvability of a system, since perturbations and mutations can occur within a module with minimal effects on the whole system [19]. It has been proposed that modularity facilitates evolutionary change by allowing new connections to be made between modules without disrupting the core function of the modules [66]. Modularity has been observed in many networks [67,68]. The modules of metabolic networks have bow-tie structure, just like the networks themselves [21]; that is, bow-tie architecture can be nested.

In the gene regulatory network of male tail tip morphogenesis, we find evidence for many conserved regulatory and effector modules. Regulatory modules include Hox patterning, the sex-determination and heterochronic pathways and TGF-β signaling. We also identified tail tip roles for additional Wnt pathway components, i.e. the SYS-1 beta-catenin, the MIG-1 Frizzled-like receptor, and the LIT-1 Nemo-like MapK. Effector modules consist of conserved components controlling vesicular trafficking and endocytosis, establishment of cellular polarity, cytoskeletal rearrangement, and cellular fusion.

Degeneracy

Degeneracy describes the coexistence of structurally or mechanistically different components that can perform similar roles or are interchangeable under certain conditions [64]. Degeneracy confers robustness because, in a system composed of partially redundant elements, one element can compensate for the failure of another. One mechanism that generates degeneracy is gene duplication. In the male tail tip morphogenesis system, we find several examples for degeneracy due to gene paralogy. We think that MAB-3 and DMD-3 function partially redundantly because the phenotype of the *mab-3(e1240);dmd-3(ok1327)* double mutant is more severe than that of *dmd-3(ok1327)* or *mab-3(e1240)* alone [7]. Similarly, two other pairs of paralogs function semi-redundantly: the Hox genes *php-3* and *nob-1* and the GATA transcription factors *egl-18* and *elt-6*, which form an operon. In both cases, removal of both genes results in a much more severe disruption of morphogenesis than removal of only one gene.

Both modularity and degeneracy contribute in a major way to the robustness of a system [19]. Indeed, the majority of RNAi

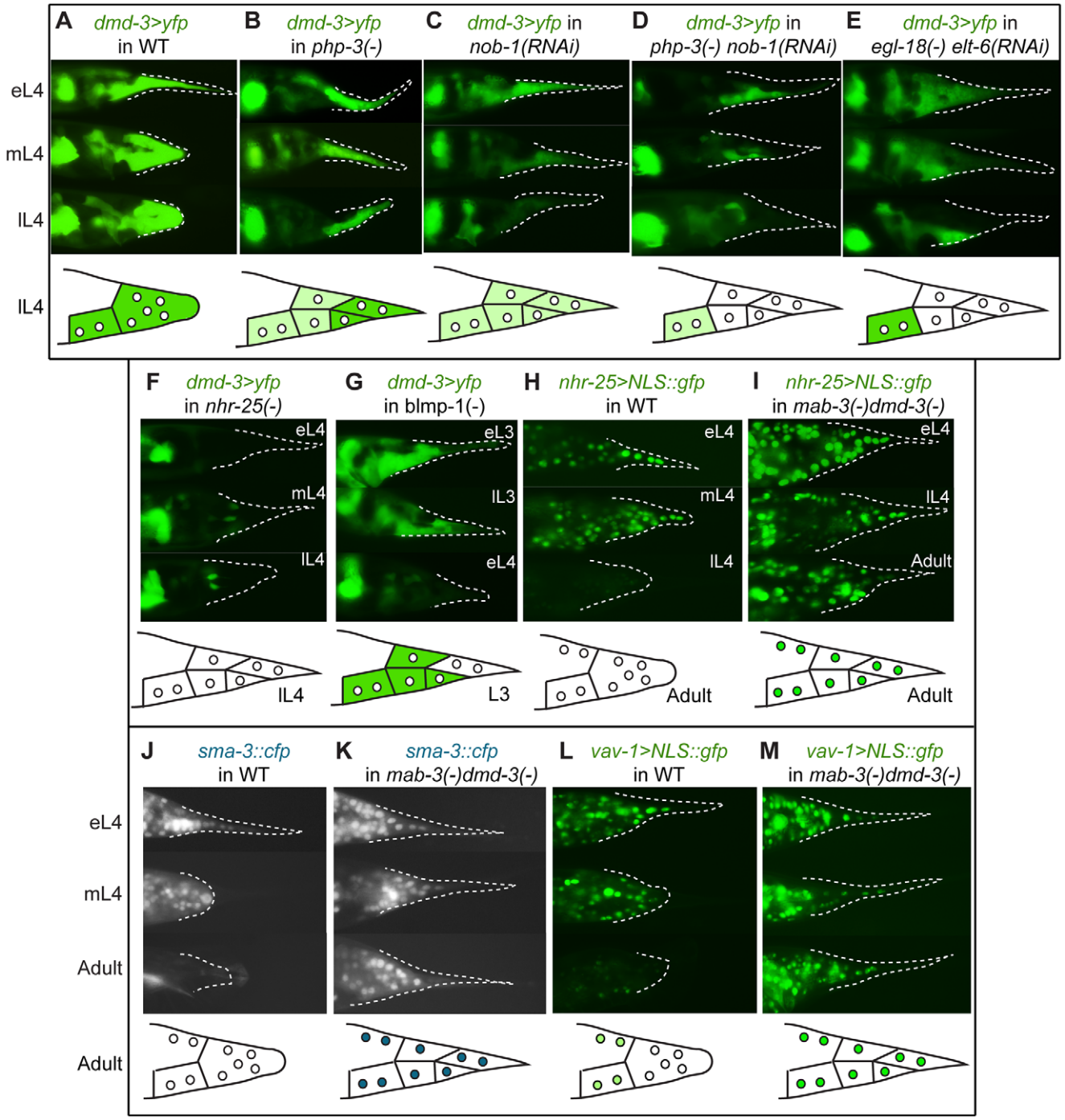

Figure 6. Expression epistasis experiments to test interactions between key regulatory genes. In the top of each panel are fluorescent micrographs of male tails (lateral views) at three of several stages (eL3 = early L3, lL3 = late L3, eL4 = early L4, mL4 = mid-L4, lL4 = late L4, or adult) expressing various transgenes in different genetic backgrounds. At the bottom of each panel is a schematic depicting the expression pattern at one exemplar stage. (A) Expression of a *dmd-3>yfp* transcriptional reporter in wild-type males. (B–G) Effects on the expression of *dmd-3>yfp* by RNAi-depletion or mutations of other genes (note that tail tip morphogenesis is impaired in these RNAi-treated or mutant males and rounding of the tail tip in lL4 does not occur). (B) Loss of *php-3* function in *ok919* mutant animals causes reduced *dmd-3>yfp* expression in hyp8, hyp11 and hyp13. (C) Depletion of *nob-1* by RNAi causes reduced *dmd-3>yfp* expression in hyp8–11. (D) *php-3(ok919) nob-1(RNAi)* animals show no *dmd-3>yfp* expression in hyp8-11. (E) Although *dmd-3>yfp* is initially expressed in *egl-18(ok290) elt-6(RNAi)* animals, it shuts off prematurely in hyp8–11. (F) Expression of *dmd-3>yfp* is never initiated in the tail tip cells of *nhr-25(ku217)* reduced-function mutants. (G) *blmp-1(tm548)* mutants show precocious expression of *dmd-3>yfp* in eL3 in hyp8, hyp9 and hyp11, no expression in hyp10, and premature inactivation of *dmd-3>yfp* at early L4. (H) *nhr-25>NLS::gfp* is expressed brightly prior to and at the beginning of morphogenesis and is quickly inactivated near its end. (I) In *mab-3(e1240);dmd-3(ok1327)* animals, expression of the *nhr-25* reporter remains bright in adult males. (J) SMA-3::CFP is expressed and nuclearly localized in hyp8–11 during morphogenesis and is not visible in adult males (the image shows autofluorescence of the spicules and the fan). (K) In *mab-3(e1240);dmd-3(ok1327)* adults, expression of the *sma-3::cfp* reporter remains very bright into adulthood. (L) *vav-1>NLS::gfp* is expressed brightly in hyp8–11 and in other cells of the tail prior to and during morphogenesis and at extremely low levels in adults. (M) Expression of the *vav>NLS::gfp* reporter remains very bright in hyp8–11 and the other cells of the male tail in adult *mab-3(e1240);dmd-3(ok1327)* animals.
doi:10.1371/journal.pgen.1002010.g006

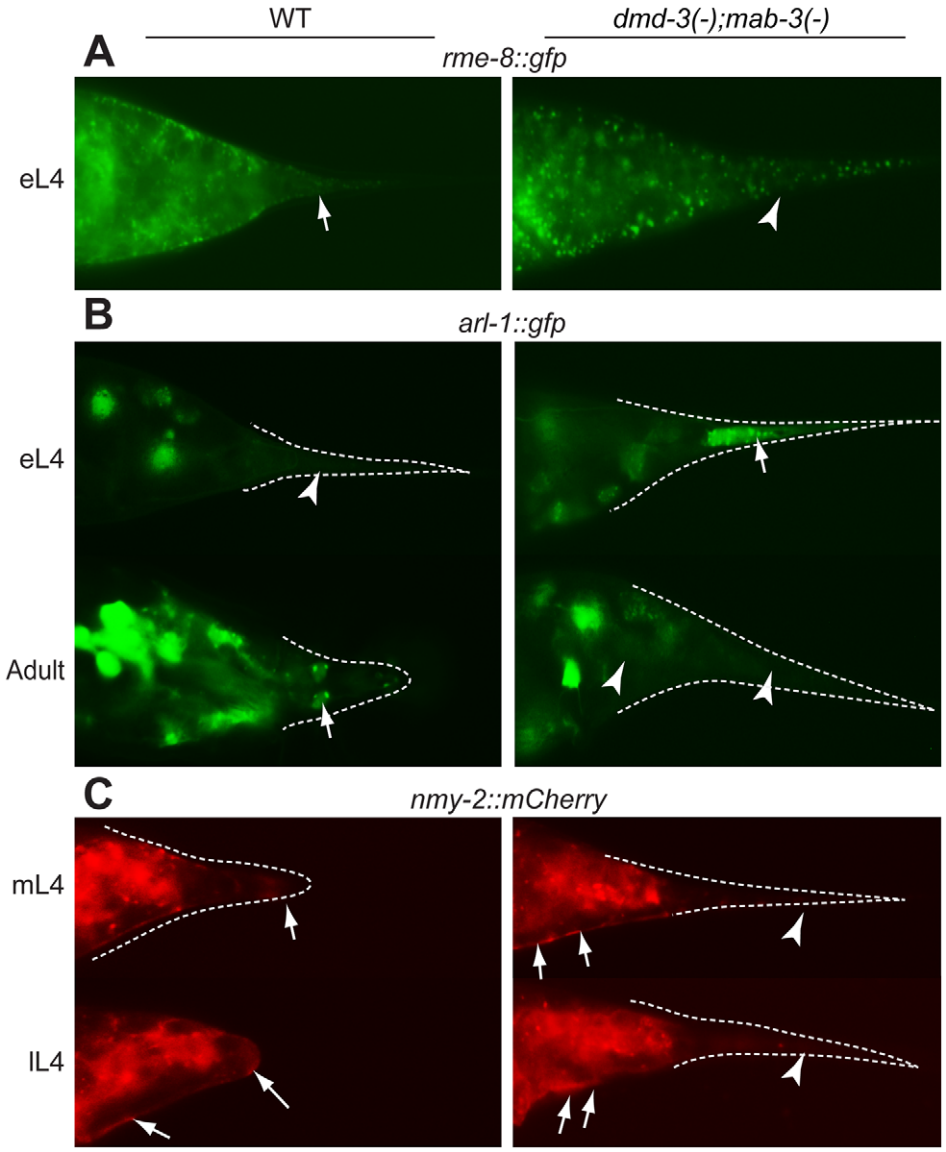

Figure 7. Cellular processes controlled by DMD-3 and MAB-3. Expression patterns of translational fusions are shown for wild-type males (left side of each panel) and *mab-3(e1240);dmd-3(ok1327)* mutant males (right side of each panel). (A) DMD-3 and MAB-3 regulate RME-8 localization but not expression. In wild-type animals, RME-8::GFP localizes as discrete puncta to the cell cortex where the tail tip cells are detaching from the cuticle (arrow), but is dispersed and cytoplasmic (arrowhead) in *mab-3(e1240);dmd-3(ok1327)* mutants. (B) In early L4, ARL-1::GFP shows very low levels of expression in wild-type males (arrowhead) but bright expression in hyp10 (arrow) in *mab-3(e1240);dmd-3(ok1327)* males. In adults, ARL-1::GFP is expressed in tail neurons in wild-type males (arrow points to phasmids), but not in *mab-3(e1240);dmd-3(ok1327)* males (arrowheads). (C) In wild-type males, NMY-2::mCherry localization is focused to a cap at the posterior end of the tail tip during rounding and to the region along the ventral edge where the tail tip cells are detaching from the cuticle (arrows). In *mab-3(e1240);dmd-3(ok1327)* animals, localization to the ventral surface still occurs (arrows), but localization to the posterior end of the tail is not observed (arrowheads).
doi:10.1371/journal.pgen.1002010.g007

knockdown phenotypes suggest that male tail tip morphogenesis is very robust against genetic perturbations. In most cases, the effects of RNAi (as well as some of the mutations tested) were subtle and the penetrance was low, suggesting that there is extensive buffering of the system against partial depletion of individual transcripts (or reduced functionality of genes).

Bow-tie network architecture

The conserved core. A role for *dmd-3* as a central regulator of male tail tip morphogenesis has been proposed previously [7]. This gene is required for male tail tip morphogenesis and, when misexpressed in the hermaphrodite tail tip, is sufficient to cause ectopic morphogenesis [7]. Another DM-domain gene, *mab-3*, has a partially redundant role with *dmd-3* in tail tip morphogenesis. We propose that the conserved core contains both of these genes as well as the gene for the nuclear hormone receptor NHR-25. NHR-25 is a highly conserved protein which in other contexts cooperates with pathways involved in tail tip morphogenesis. NHR-25 interacts with the Wnt pathway during asymmetric division of the T cell [57], and with the Hox protein NOB-1 during embryogenesis [59]. There is also evidence that *nhr-25* is connected to the heterochronic pathway, as it is a target of the miRNA *let-7* [58]. *nhr-25* is the only gene we have found to be required for the initiation and not just the maintenance of *dmd-3*

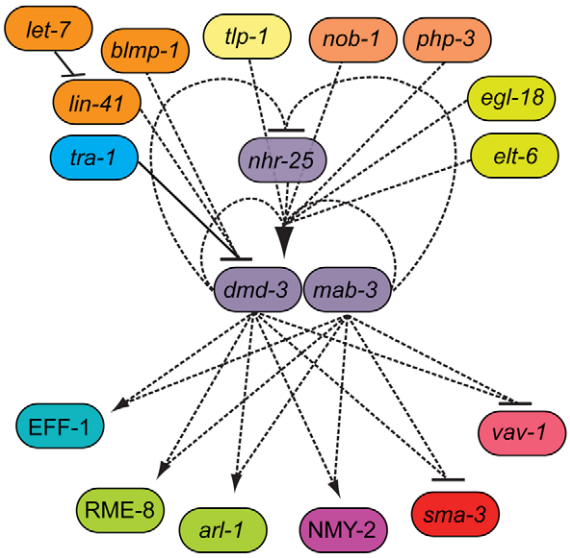

Figure 8. The genetic architecture of tail tip morphogenesis, showing experimentally validated connections between components. This network has a bow-tie architecture with *dmd-3, mab-3* and *nhr-25* in the core. The central role for *dmd-3* and *mab-3* was originally proposed by Mason et al. [7]. We found that *nhr-25* is required for the activation of *dmd-3* and forms a negative feedback loop with *dmd-3* and *mab-3*. Multiple signaling pathways/genes feed into the core by regulating *dmd-3* positively (lines with arrow at one end) or negatively (lines with bar at one end). Genes controlling morphogenesis (*rme-8, nmy-2, arl-1, eff-1*) and other signaling pathways (TGF-β and *vav-1*-mediated) are regulated by *dmd-3* and *mab-3*. Dashed lines indicate possibly direct or indirect interactions, solid lines indicate an experimentally validated direct interactions [7].
doi:10.1371/journal.pgen.1002010.g008

expression. *dmd-3* expression is completely eliminated in *nhr-25(ku217)* mutants and complete removal of *nhr-25* (e.g. *nhr-25 RNAi* performed on the *nhr-25(ku217)* hypomorphic strain) results in the same phenotypes as the *mab-3(e1240);dmd-3(ok1327)* double mutant. *dmd-3/mab-3* and *nhr-25* regulate each other through a feedback loop. Thus, these three genes probably form a module in the core of the network.

Inputs to the core. Input from multiple modules regulates the sex-specific, spatial, and temporal expression of the core gene *dmd-3*. Sex-specificity is provided by the most downstream component of the sex-determination pathway, TRA-1, which inhibits expression of *dmd-3* in hermaphrodites [7]. Previous studies [5,7] have proposed that Wnt signaling provides spatial information. We found evidence that Hox and GATA factors also contribute to spatial patterning. Hox genes are known to govern patterning along the anteroposterior axis. As is expected, the genes involved in tail tip morphogenesis, *nob-1* and *php-3* are the most posterior Hox genes in *C. elegans* [69]. The GATA transcription factors *egl-18* and *elt-6* are excluded from the tail tip cells but are expressed in all the neighboring cells. They are nevertheless required for tail tip morphogenesis. We therefore postulate that GATA factors provide positional information through signaling from neighboring cells.

The heterochronic pathway provides temporal input, which ensures that morphogenesis occurs during the correct time window during the L4 stage. Overexpression of *lin-41* and deletion of *let-7* lead to delayed morphogenesis; removal of *lin-41* leads to precocious tail tip retraction [6]. We propose here that *blmp-1* is also a component of the heterochronic pathway, because removing *blmp-1* results in precocious expression of *dmd-3* and in precocious tail tip retraction. We are currently determining where *blmp-1* acts in the heterochronic pathway.

Outputs from the core. In the tail tip system, the output downstream of the conserved core involves effectors of morphogenesis. One such output is cellular fusion driven by the fusogen protein EFF-1 [3,7,15,16]. In addition, our screen has shown that genes involved with vesicular trafficking, endocytosis, establishment of cellular polarity, cytoskeletal rearrangement, cell-cell communication and transport are on the output side of the bow tie. Electron microscopy revealed an accumulation of vesicles during male tail tip morphogenesis, suggesting an important role for trafficking [3]. Consistent with this observation, two genes involved in vesicular trafficking and endocytosis that were identified in the screen display dynamic expression or localization patterns during tail tip morphogenesis: *arl-1*, which encodes an ADP-ribosylation factor [70,71], and *rme-8*, which encodes a J-domain protein vital for receptor-mediated endocytosis [52]. Trafficking and endocytosis have been shown to play a key role in morphogenesis in other systems. For example, endocytosis of cadherins is required for the morphogenetic movement during *Xenopus* gastrulation [72] and the anterior migration of prechordal plate cells in zebrafish [73,74]. The severity of the tail tip phenotype indicates that endocytosis, controlled by RME-8, is an essential process for tail tip morphogenesis. Removing *rme-8* postembryonically, by either RNAi or with a temperature-sensitive allele, results in a complete failure of tail tip morphogenesis. Also, RME-8 localizes to regions of the plasma membrane which undergo dynamic change: the ventral border of the tail tip cells as they detach from the L4 cuticle, and the posterior edge of the rounding cells. This pattern is consistent with a proposed role for RME-8 during early endosome membrane trafficking and receptor recycling [61,75,76]. It has been observed that, in the absence of RME-8, components of signaling pathways (e.g. Wnt) that should be recycled to the membrane are instead shuttled to the lysosome and degraded [61]. It is therefore possible that RME-8 influences signaling events required for tail tip retraction which cannot occur in the absence of receptor recycling.

Morphogenesis in all systems likely involves the rearrangement of an acto-myosin network to drive cell movement and shape change. Our data suggest that, in the tail tip, these processes are controlled by CDC-42, a highly conserved Rho-GTPase [77], and NMY-2, a non-muscle myosin. Our expression analysis is consistent with NMY-2 playing a key role in reshaping the pointed tail tip cells into a rounded syncytium. NMY-2 localization to a cap at the end of the tail tip is reminiscent of what has been observed during *C. elegans* gastrulation where NMY-2 localizes to the apical surface of the ingressing E daughter and MS descendant cells [78]. Additionally, at the start of tail tip retraction, we observed clear foci of NMY-2 at the apical surfaces with fibrous NMY-2 densities projecting from the apical foci inside the tail tip cells. This organization is strikingly similar to the arrangements of non-muscle myosin observed for apical constriction during *Drosophila* gastrulation in which the apical surface area is constricted by a ratchet-like contraction of an actin network [79]. Similarly, CDC-42 localizes to foci at the apical boundaries of the tail tip cells, where it could have a role in activating the formation of actin filaments required for such "apical constriction."

Gap junctions are required for epithelial morphogenesis during embryogenesis in *Drosophila* [80] and play a role during the cellular changes of metastasis, such as cellular migration [81]. INX-12 and INX-13 connect the cytoplasm of neighboring cells through the formation of gap junctions [82] and are required for tail tip

morphogenesis. Oddly, our reporters show their peak of expression when the tail tip cells have already fused. It is possible that these innexins are forming new gap junctions between the tail tip and other cells and that these junctions are required for efficient or continued retraction/migration.

Versatile weak linkages. Kirschner and Gerhart [83] define versatile weak linkage in biological systems as a kind of regulatory connection that can be easily broken or redirected for other functions during evolution or development. In bow-tie networks, the interfaces between input, core, and output are formed by weak linkages. Examples of components that can establish versatile weak linkages include second messengers, G-proteins, and the transcription machinery [84]. On the input side of the tail tip regulatory network, we have identified many transcription factors and signaling pathways. The control of *dmd-3* transcription involves many of these inputs. It is thus possible that each input forms a weak interaction with *dmd-3*. One example of a weak linkage that might connect the core to the output is CDC-42, a Rho-GTPase which integrates multiple signaling pathways to mediate cellular responses [19,85]. Additionally, processes involved in post-transcriptional gene regulation have attributes of weak linkage. We identified genes that encode for RNA splicing factors, kinases, phosphatases, proteases, ubiquitinating and neddylating proteins, and other enzymes with the capacity for post-translational modification of the cytoskeleton or other parts of the cellular machinery. One example of the latter is UBC-12, a ubiquitin-conjugating enzyme that produced a strong phenotype and was expressed throughout but not prior to tail tip morphogenesis. The fusogen-encoding gene *eff-1* that is required for cell fusion may also be regulated post-transcriptionally. It has been shown that DMD-3 and MAB-3 do not influence *eff-1* transcription, but they positively regulate EFF-1 protein levels [7]. Similarly, we show that DMD-3 somehow regulates the localization of RME-8 and NMY-2, but not their expression.

System controls. One feature of bow-tie networks is system control, consisting of positive and/or negative feedback which can occur between components at all levels of the network [19]. Precise system control has been emphasized as an important aspect of developmental systems since precision, robustness and versatility are stringent requirements in development and errors are particularly serious [86]. Positive autoregulation occurs when a transcription factor either directly or indirectly activates its own expression which results in the maintenance of transcription in the absence of the factors that initiated expression. Positive feedback can be used in temporal control to sustain expression over a developmental period, or in spatial control to restrict expression to a specific region [86,87]. Patterning and duration of expression are also influenced by negative autoregulation where, for example, a transcription factor directly or indirectly represses its own expression [86,87].

Both DMD-3 and MAB-3 are required for maintaining the expression of *dmd-3*, thus forming a positive feedback loop [7]. We show here that these genes are also involved in a negative feedback loop, since they inhibit NHR-25 in a pathway which regulates their own expression. We propose that these feedback loops are important for regulating the duration of morphogenesis. Specifically, the regulatory loop between NHR-25 and MAB-3/DMD-3 appears to play a key role in the temporal regulation of morphogenesis. After *dmd-3* expression is initiated, its product inhibits NHR-25 production, probably in combination with translational inhibition of *nhr-25* by *let-7* miRNA [58]. This mechanism should prevent the kind of over-retraction (Ore) phenotype seen in *lin-41(ma104*lf*)* mutants in which *dmd-3* is on for too long because its expression begins precociously in L3 and continues through L4. The specific mechanisms of this feedback loop are a topic of further study in our lab.

Another system control mechanism involves the TGF-β pathway and VAV-1. As positive regulators of morphogenesis, we would expect these pathways to either positively regulate or be positively regulated by DMD-3. However, DMD-3 and MAB-3 negatively regulate these pathways. These interactions might function to restrict morphogenesis in time and space. How this regulation is facilitated is still unknown.

In summary, we have presented evidence that the genetic network underlying *C. elegans* male tail tip morphogenesis is consistent with a bow-tie architecture in which *dmd-3, mab-3* and *nhr-25* are the central regulators in a conserved core (Figure 8). Of the 23 different interactions we tested by expression epistasis, 11 showed an epistatic effect on expression or localization; all of these involved *dmd-3* and/or *mab-3*. Twelve interactions showed no effects; of these, only four involved *dmd-3* and/or *mab-3* (Table S5). We therefore believe that the position of *dmd-3* and *mab-3* in the core of the network is real and not merely an effect of a bias in our experimental design.

Conclusion

The architecture of the genetic network regulating male tail tip morphogenesis in *C. elegans* is congruent with the bow-tie model, since we find evidence for all the characteristics of bow-tie networks. We find modularity, degeneracy, a conserved core, weak linkage and positive and negative feedback loops connecting spatial, sexual and temporal inputs to the cellular responses required for morphogenesis. To our knowledge, this is the first time that a genetic network regulating a morphogenetic process has been specifically investigated for bow-tie architecture. However, it is likely that other morphogenetic events—e.g., the development of the eye in flies and possibly mammals and the formation of the pharynx in *C. elegans*—are also controlled by bow-tie regulatory networks. In both examples, components have been identified which are likely to be part of the conserved core. *Drosophila* eye development is in part controlled by the products of eight eye specification genes. Deletion of either one of these genes leads to a drastic reduction or loss of the adult eye, whereas ectopic expression of all but one results in retinal development outside of normal eye tissue [88,89]. The fly eye specification genes are conserved with orthologs in mammals. Expression of one of them, *dachshund*, is regulated by at least 36 upstream factors, including the TGF-β signaling pathway, the transcription factor Zerknüllt and several other patterning genes (e.g. *krüppel*, *snail* and *dorsal*) [88], suggesting the existence of an extensive input fan in this system. The FoxA transcription factor PHA-4 is a central regulator of pharynx development in *C. elegans*. *pha-4* is the only zygotic gene that deletes the entire pharynx when mutated [90]. FoxA transcription factors are conserved from Cnidaria to mammals and are always associated with the digestive tract [90]. PHA-4 has hundreds of targets, many of which are directly regulated at the transcriptional level [91,92]. In this system, feedback loops have been identified as well [90]. Thus, there is evidence for a conserved core, an output fan and system control as elements of a bow-tie network architecture for pharynx morphogenesis. Finding bow-tie networks in multiple developmental systems supports the notion that this architecture is a universal feature of evolved gene regulatory networks and is favored by selection due to its robustness. The male tail tip thus provides a simple model for investigating not only morphogenetic mechanisms, but also the properties of a universally important genetic regulatory architecture.

The evolvable male tail. One general advantage of bow-tie architecture is the ease with which it can accommodate

evolutionary changes (evolvability). Weak linkage allows the addition, deletion or switching of components without disturbing the entire system [93–95]. The prediction, therefore, is that a comparison of the genetic architecture for a particular process in different species will uncover differences primarily in the input or output fan of the bow-tie network, but not in the core or the conserved components of the interface. The male tail of nematodes related to *C. elegans* is a great model in which to study network architecture in an evo-devo context and test this prediction. One attractive aspect of the male tail tip in an evolutionary context is that it has changed shape repeatedly in multiple lineages [96,97], thus providing a model not only to uncover the genetic architectural changes underlying the evolution of morphogenesis, but also to test if the same or different parts of the genetic architecture are altered in repeated emergences of similar morphologies. Future research will thus be focused on building a more complete picture of male tail tip regulatory architecture in *C. elegans* and developing genomic methods to allow comparisons with related species.

Materials and Methods

Strains and transgenic lines

Genetic manipulations and culturing of *C. elegans* were performed as previously described [98]. We use the following nomenclature for transgenes (similar to that used by Ziel et al. [99]). Transcriptional reporters are designated by the name of the gene associated with the promoter, followed by a ">" and the reporter gene to which it is fused (e.g., *dmd-3>yfp*). Translational reporters are designated by the gene, followed by "::" and the reporter to which it is fused (e.g., *sma-3::mCherry*). Unless otherwise stated, the endogenous promoter is used to drive expression of translational reporters. If a different promoter is used, we use both designations (e.g., *lin-44>php-3::gfp* represents the *php-3* gene fused to the *gfp* gene, with expression driven by the promoter of the *lin-44* gene). Unless otherwise stated, the *unc-54* 3′UTR is used for all constructs. The protein product of a construct is designated with capital letters (e.g., PHP-3::GFP). No construct employed cDNA; all introns were included.

Strains with transgenes generated for this paper are listed in Table S3. Other strains used for this study are listed below.

CB4088 = *him-5(e1490)V*. This is the otherwise wild-type, male-producing strain used as the background genotype in this study (from Caenorhabditis Genetics Center, CGC).

BW2020 = *ctIs57[nob-1::gfp + rol-6]* (a gift from Zhongying Zhao, University of Washington, Washington). Hermaphrodites of this strain were crossed with CB4088 males to obtain a *him-59(e1490)V; ctIs57* strain.

DF125 = *php-3(ok919)III; him-5(e1490)V*. Made by crossing CB4088 males with RB998 hermaphrodites. RB998 = *php-3(ok919)III* (from CGC).

DF159 = *rme-8(b1023)I; him-5(e1490)V*. Made by crossing CB4088 males with DH1206 hermaphrodites. DH1206 = *rme-8(b1023)I* (from CGC).

DF160 = *blmp-1(tm548)I; him-5(e1490)V; fsIs3[dmd-3>yfp + unc-122>gfp]*.

DF161 = *blmp-1(tm548)I; him-5(e1490)V*. Made by crossing CB4088 males with hermaphrodites carrying the *blmp-1(tm548)* allele (from Shohei Mitani, National BioResource Project, Tokyo Women's Medical University School of Medicine, Tokyo, Japan).

DF163 = *sma-3(e491)III; him-5(e1490)V*. Made by crossing CB4088 males with CB491 hermaphrodites. CB491 = *sma-3(e491)III* (from CGC).

DF164 = *egl-18(ok290)IV; him-5(e1490)V*. Made by crossing CB4088 males with JR2370 hermaphrodites. JR2370 = *egl-18(ok290)IV* (from CGC).

DF167 = *him-5(e1490)V; nhr-25(ku217)X*. Made by crossing CB4088 males with MH1955 hermaphrodites. MH1955 = *nhr-25(ku217)X* (from CGC).

DF171 = *him-5(e1490)V; bIs34[rme-8::gfp + rol-6]*. Made by crossing CB4088 males with DH1336 hermaphrodites. DH1336 = *bls34[rme-8::gfp + rol-6]* (from CGC).

DF177 = *him-5(e1490)V; nhr-25(ku217)X; fsIs3[dmd-3>yfp + unc-122>gfp]*.

DF178 = *mab-3(e1240)II; dmd-3(ok1327) him-5(e1490)V; bIs34[rme-8::gfp + rol-6]*.

DF196 = *him-5(e1490)V; xnIs8[pJN343: nmy-2::mCherry + unc-119(+)]*. This strain was made by crossing CB4088 males to hermaphrodites carrying the transgene *xnIs8* which were a generous gift from Jeremy Nance (NYU Skirball Institute, New York, New York).

DF197 = *mab-3(e1240)II; dmd-3(ok1327) him-5(e1490)V; xnIs8[pJN343: nmy-2::mCherry + unc-119(+)]*.

DF199 = *ptl-1(ok621)III; him-5(e1490)V*. Made by crossing CB4088 males to RB808 hermaphrodites. RB808 = *ptl-1(ok621)III* (from CGC).

JJ1473 = *unc-119(ed3)III; zuIs45[nmy-2::gfp + unc-119(+)]* (from CGC).

KC447 = *rrf-3(pk1426)II; him-5(e1490)V*. A generous gift from King L. Chow (Hong Kong University of Science and Technology, Hong Kong, China).

KC529 = *eri-1(mg366)IV; him-5(e1490)V*. (from K. L. Chow).

UR157 = *fsIs2[dmd-3>yfp + unc-122>gfp]I?; him-5(e1490)V*. A generous gift from Douglas Portman (Rochester University, New York).

UR279 = *mab-3(e1240)II; dmd-3(ok1327) him-5(e1490)V* (from D. Portman).

WM79 = *rol-6(n1270)II; neEx[lit-1::GFP + rol-6(su1006)]* (from CGC). Hermaphrodites of this strain were crossed with CB4088 males to obtain a *rol-6(n1270)II; him-5(e1490)V; neEx[lit-1::GFP + rol-6(su1006)]* strain.

RNAi screen

The genome-wide RNAi-feeding screen was carried out in the RNAi-hypersensitive background *rrf-3; him-5* (strain KC447). RNAi effects on embryogenesis were bypassed by feeding siRNA-expressing bacteria to synchronized L1 larvae. Following a recommendation by K. Chow (pers. comm.), L1 larvae were plated onto a thin film of agar (1.5 ml per 60 mm plate) containing 2 mM IPTG and 100 µg/ml ampicillin. Worms were cultured to adulthood (3 days) at 20°C at which time a square of agar with worms was removed and mounted directly onto a glass slide and covered with a coverslip (Figure 1A). All scoring was carried out at 400x with a Zeiss Axioskop equipped with Nomarski differential interference contrast. Images were recorded with a C4742-95 "Orca" Hamamatsu digital camera and Openlab software, ver. 3.0.9 (Improvision). The secondary screen was carried out in the same way but in a different RNAi hypersensitive background, *eri-1* (strain KC529). RNAi clones consistently conferring a Lep or Ore tail tip phenotype were sequenced to confirm the targeted genes. All scoring data and images are available via our male tail tip database, MTTdb, at http://wormtails.bio.nyu.edu.

Generation of transgenic strains

Translational fusions and transcriptional reporters were constructed by overlap-extension PCR as previously described [100]. The 5′ upstream sequence and coding sequences for *php-3* (-500 bp to the

stop codon), *egl-18* (-3691 to stop), *rcn-1* (-4797 to stop), *ptl-1* (-2105 to stop), *arl-1* (-550 to stop), *abcx-1* (-437 to stop), *cdc-42* (-1814 to stop), *sys-1* (-3411 to stop), *inx-12* (-3975 to stop), *blmp-1* (-4916 To stop), *nhr-165* (-1559 to stop), and *ubc-12* (-363 to stop), were PCR-amplified from genomic DNA and fused to *gfp* and the *unc-54* 3′-UTR amplified from pPD95.75 (Addgene). The 5′-upstream sequence and coding region of *sma-3* (from -1169 bp), amplified from genomic DNA, was fused to *mCherry* [101] and to *cfp*, which were PCR-amplified from pGC326 (a gift from E. J. Hubbard) and pPD136.61 (Addgene), respectively. To make the DAF-4 reporters, the upstream sequence and coding region (from -5091) was fused to *yfp* that was amplified from pPD136.64 (Addgene). A transcriptional reporter of *daf-4* fused the upstream sequence (-4865 to -1) to the NLS and *gfp* amplified from pPD122.13 (Addgene). The transcriptional reporter for *nhr-25* fused the upstream sequence (-9100 to -1) to the NLS and *gfp* from pPD122.13 (Addgene) followed by the 3′-UTR for *nhr-25* (stop to +760 bp). Transcriptional reporters for *inx-12* (-3975 to -1) and *inx-13* (-1557 to -1) were fused to *yfp* (pPD136.64 (Addgene)) and *cfp* (pPD136.61(Addgene)).

Transgenes were microinjected at concentrations ranging from 5–20 ng/µl along with 100 ng/µl pRF4 (*rol-6(su1006)*) as injection marker. Multiple lines were analyzed for each construct using epifluorescence (Axioskop with mercury lamp, 400 or 1000x). Representative images of fluorescence expression patterns are available via the MTTdb database at http://wormtails.bio.nyu.edu. Strain names and primer sequences are provided in Table S3.

Network model-building

Genes identified in our screen were manually entered into N-Browse2 (http://Aquila.bio.nyu.edu/NBrowse2/nbrowsetest.jnlp) [17]. Only a subset of these genes showed annotated interactions, and only those with an interaction one or two edges away from another candidate gene were added to our network (Figure 5). Information from other studies [6,7,44,51,57–60] which show genetic or direct interactions with known or newly identified tail tip genes were also included (Figure 5).

Supporting Information

Figure S1 RNAi phenotypes of some genes are very similar to the phenotypes of null mutants. (A,C,E,G) Lep phenotypes generated by RNAi-knockdown of *php-3, egl-18, sma-3,* and *nhr-25,* respectively. (B,D,F,H) Null mutants of the same genes with similar Lep phenotypes. Arrows point to the Lep tails.
(PDF)

Figure S2 Driving expression of PHP-3::GFP with a *lin-44* promoter in hyp8–11 only is sufficient to rescue the Lep phenotype of *php-3(ok919)* males. Fluorescent micrographs are shown on the left and DIC images of the same animals on the right sides of each panel. (A) Tail tip-specific expression of *lin-44>php-3::gfp* is observed throughout tail tip morphogenesis and into adulthood, similar to *lin-44* reporter and *in situ* expression patterns described previously [25]. DIC images show normal tail tip retraction. The temporary appearance of a small bubble during the rounding of the tail tip cells is a normal variation commonly seen in wild-type animals. Adult animals have normal, rounded tail tips (arrow) never seen in the *php-3(ok919)* background. (B) Mosaics in which only a subset of the tail tip cells expresses the *php-3::gfp* transgene (arrows in left panels) fail to rescue the Lep phenotype (arrows in right panels).
(PDF)

Figure S3 RNAi phenotype and expression pattern of translational reporters for a selection of genes positive in the RNAi screen. (A) RNAi of the nuclear hormone receptor gene *nhr-165* resulted in Lep phenotypes (arrow). NHR-165::GFP is not expressed in hyp8–11 (arrowhead), but is expressed in surrounding hypodermal cells. (B) RNAi against the ubiquitin conjugating enzyme gene *ubc-12* results in Lep tails (arrow). UBC-12::GFP is expressed intensely in early L4 males in hyp10 (arrow) but is not seen in all animals (arrowhead pointing to the tail tip of a different animal). (C) RNAi of the beta-catenin gene *sys-1* resulted in Lep phenotypes. SYS-1::GFP is localized in the cytoplasm of hyp8 and hyp11 during early L4 (arrows) but not in hyp9 or hyp10 (arrowheads). (D) RNAi of the MapK gene *lit-1* resulted in Lep phenotypes (arrow). LIT-1::GFP is localized to the nuclei of hyp9 and hyp10 (arrows) but not hyp8 or hyp11 (arrowheads) during tail tip morphogenesis.
(PDF)

Figure S4 Expression pattern of a translational reporter for non-muscle myosin 2, NMY-2::GFP. During tail tip morphogenesis (mL4 = mid-L4), foci of NMY-2::GFP are observed at the apical surfaces of the migrating tail tip cells (arrowheads). An NMY-2::GFP cap forms at the posterior surface of the migrating tail tip cells (arrows), and later (lL4 = late L4) along the ventral surface of the entire male tail.
(PDF)

Table S1 Genes identified in the RNAi screen for tail tip defects in *C. elegans*. L = Lep RNAi phenotype, O = Ore-like RNAi phenotype, O+L = both phenotypes. Penetrance (number of worms scored showing the phenotype) for the Lep phenotype is indicated by asterisks as follows: * = 1–2 males with the RNAi phenotype ** = 3–5 males, *** = >5 males). Severity (* = short rounded ("knobby") Lep tail tips only, ** = short rounded ("knob") and long pointed tail tips, *** = only long pointed Lep tail tips). Ore phenotypes were always severe (***). Penetrance data for all genes scored are available via the MTTdb database at http://wormtails.bio.nyu.edu.
(DOCX)

Table S2 Mutant phenotypes of genes identified in the genome-wide RNAi screen.
(DOCX)

Table S3 Transgenic strains and primers used to construct the transgenes.
(DOC)

Table S4 RNAi experiments that could not be scored due to larval lethality.
(DOCX)

Table S5 Genetic interactions tested by expression epistasis.
(DOCX)

Video S1 Non-muscle myosin 2 localization in an early L4 male. NMY-2::GFP forms a cap at the cell cortex at the posterior end of the tail tip syncytium as it is rounding and changing shape. NMY-2::GFP can also be seen at the tips of the developing rays.
(MOV)

Video S2 Non-muscle myosin 2 localization in a mid- L4 male. NMY-2::GFP localizes to the cell cortex along the ventral surface of the developing male tail, as well as at the tips of the developing rays.
(MOV)

Acknowledgments

We thank the Fitch lab members who assisted in this work: Emily Peitzman, Ellen Vickery, and Anita Anburajan. We also thank the Caenorhabditis Genetics Center, the National BioResource Project (S. Mitani, Tokyo Women's Medical University), Dr. King L. Chow, Dr. Jane Hubbard, Dr. Adam Mason, Dr. Jeremy Nance, Dr. Doug Portman, and Dr. Zhongying Zhao for valuable strains, reagents and critiques of the manuscript.

Author Contributions

Conceived and designed the experiments: MN DF. Performed the experiments: MN EZ. Analyzed the data: MN. Wrote the paper: MN KK DF. Technical help: KK, HF, GM, DM, KS.

References

1. Hadjantonakis K, Solnica-Krezel L (2010) Developmental biology 50 years-investigating the emergence of shape. Introduction. Dev Biol 341: 2–4.
2. Sulston JE, Albertson DG, Thomson JN (1980) The *Caenorhabditis elegans* male: postembryonic development of nongonadal structures. Dev Biol 78: 542–576.
3. Nguyen CQ, Hall DH, Yang Y, Fitch DH (1999) Morphogenesis of the *Caenorhabditis elegans* male tail tip. Dev Biol 207: 86–106.
4. Sulston JE, Horvitz HR (1977) Post-embryonic cell lineages of the nematode, *Caenorhabditis elegans*. Dev Biol 56: 110–156.
5. Zhao X, Yang Y, Fitch DH, Herman MA (2002) TLP-1 is an asymmetric cell fate determinant that responds to Wnt signals and controls male tail tip morphogenesis in *C. elegans*. Development 129: 1497–1508.
6. Del Rio-Albrechtsen T, Kiontke K, Chiou SY, Fitch DH (2006) Novel gain-of-function alleles demonstrate a role for the heterochronic gene *lin-41* in *C. elegans* male tail tip morphogenesis. Dev Biol 297: 74–86.
7. Mason DA, Rabinowitz JS, Portman DS (2008) *dmd-3*, a doublesex-related gene regulated by *tra-1*, governs sex-specific morphogenesis in *C. elegans*. Development 135: 2373–2382.
8. Fitch DH (1997) Evolution of male tail development in rhabditid nematodes related to *Caenorhabditis elegans*. Syst Biol 46: 145–179.
9. Sudhaus W, Fitch D (2001) Comparative studies on the phylogeny and systematics of the rhabditidae (nematoda). J Nematol 33: 1–70.
10. Hodgkin J (2002) The remarkable ubiquity of DM domain factors as regulators of sexual phenotype: ancestry or aptitude? Genes Dev 16: 2322–2326.
11. Raymond CS, Shamu CE, Shen MM, Seifert KJ, Hirsch B, et al. (1998) Evidence for evolutionary conservation of sex-determining genes. Nature 391: 691–695.
12. Shen MM, Hodgkin J (1988) *mab-3*, a gene required for sex-specific yolk protein expression and a male-specific lineage in *C. elegans*. Cell 54: 1019–1031.
13. Hodgkin J (1987) A genetic analysis of the sex-determining gene, *tra-1*, in the nematode *Caenorhabditis elegans*. Genes Dev 1: 731–745.
14. Zarkower D, Hodgkin J (1992) Molecular analysis of the *C. elegans* sex-determining gene *tra-1*: a gene encoding two zinc finger proteins. Cell 70: 237–249.
15. Mohler WA, Shemer G, del Campo JJ, Valansi C, Opoku-Serebuoh E, et al. (2002) The type I membrane protein EFF-1 is essential for developmental cell fusion. Dev Cell 2: 355–362.
16. Shemer G, Suissa M, Kolotuev I, Nguyen KC, Hall DH, et al. (2004) EFF-1 is sufficient to initiate and execute tissue-specific cell fusion in *C. elegans*. Curr Biol 14: 1587–1591.
17. Kao HL, Gunsalus KC (2008) Browsing multidimensional molecular networks with the generic network browser (N-Browse). Curr Protoc Bioinformatics Chapter 9: Unit 9 11.
18. Csete M, Doyle J (2004) Bow ties, metabolism and disease. Trends Biotechnol 22: 446–450.
19. Kitano H (2004) Biological robustness. Nat Rev Genet 5: 826–837.
20. Rodriguez-Caso C, Corominas-Murtra B, Sole RV (2009) On the basic computational structure of gene regulatory networks. Mol Biosyst 5: 1617–1629.
21. Zhao J, Yu H, Luo JH, Cao ZW, Li YX (2006) Hierarchical modularity of nested bow-ties in metabolic networks. BMC Bioinformatics 7: 386.
22. Oda K, Kitano H (2006) A comprehensive map of the toll-like receptor signaling network. Mol Syst Biol 2: 2006.0015.
23. Oda K, Matsuoka Y, Funahashi A, Kitano H (2005) A comprehensive pathway map of epidermal growth factor receptor signaling. Mol Syst Biol 1: 2005.0010.
24. Krantz M, Ahmadpour D, Ottosson LG, Warringer J, Waltermann C, et al. (2009) Robustness and fragility in the yeast high osmolarity glycerol (HOG) signal-transduction pathway. Mol Syst Biol 5: 281.
25. Li CW, Chen BS (2010) Identifying functional mechanisms of gene and protein regulatory networks in response to a broader range of environmental stresses. Comp Funct Genomics: 408705.
26. Kitano H, Oda K (2006) Robustness trade-offs and host-microbial symbiosis in the immune system. Mol Syst Biol 2: 2006 0022.
27. Tieri P, Grignolio A, Zaikin A, Mishto M, Remondini D, et al. (2010) Network, degeneracy and bow tie integrating paradigms and architectures to grasp the complexity of the immune system. Theor Biol Med Model 7: 32.
28. Fraser AG, Kamath RS, Zipperlen P, Martinez-Campos M, Sohrmann M, et al. (2000) Functional genomic analysis of *C. elegans* chromosome I by systematic RNA interference. Nature 408: 325–330.
29. Berriz GF, King OD, Bryant B, Sander C, Roth FP (2003) Characterizing gene sets with FuncAssociate. Bioinformatics 19: 2502–2504.
30. Mallo M, Wellik DM, Deschamps J (2010) Hox genes and regional patterning of the vertebrate body plan. Dev Biol 344: 7–15.
31. Pearson JC, Lemons D, McGinnis W (2005) Modulating Hox gene functions during animal body patterning. Nat Rev Genet 6: 893–904.
32. Herman MA, Vassilieva LL, Horvitz HR, Shaw JE, Herman RK (1995) The *C. elegans* gene *lin-44*, which controls the polarity of certain asymmetric cell divisions, encodes a Wnt protein and acts cell nonautonomously. Cell 83: 101–110.
33. Kaneko H, Shimizu R, Yamamoto M (2010) GATA factor switching during erythroid differentiation. Curr Opin Hematol 17: 163–168.
34. Ho IC, Tai TS, Pai SY (2009) GATA3 and the T-cell lineage: essential functions before and after T-helper-2-cell differentiation. Nat Rev Immunol 9: 125–135.
35. Chou J, Provot S, Werb Z (2010) GATA3 in development and cancer differentiation: cells GATA have it! J Cell Physiol 222: 42–49.
36. Koh K, Rothman JH (2001) ELT-5 and ELT-6 are required continuously to regulate epidermal seam cell differentiation and cell fusion in *C. elegans*. Development 128: 2867–2880.
37. Koh K, Peyrot SM, Wood CG, Wagmaister JA, Maduro MF, et al. (2002) Cell fates and fusion in the *C. elegans* vulval primordium are regulated by the EGL-18 and ELT-6 GATA factors — apparent direct targets of the LIN-39 Hox protein. Development 129: 5171–5180.
38. Ikushima H, Miyazono K (2010) TGFbeta signalling: a complex web in cancer progression. Nat Rev Cancer 10: 415–424.
39. Gissendanner CR, Sluder AE (2000) *nhr-25*, the *Caenorhabditis elegans* ortholog of ftz-f1, is required for epidermal and somatic gonad development. Dev Biol 221: 259–272.
40. Guichet A, Copeland JW, Erdelyi M, Hlousek D, Zavorszky P, et al. (1997) The nuclear receptor homologue Ftz-F1 and the homeodomain protein Ftz are mutually dependent cofactors. Nature 385: 548–552.
41. Yu Y, Li W, Su K, Yussa M, Han W, et al. (1997) The nuclear hormone receptor Ftz-F1 is a cofactor for the *Drosophila* homeodomain protein Ftz. Nature 385: 552–555.
42. Broadus J, McCabe JR, Endrizzi B, Thummel CS, Woodard CT (1999) The *Drosophila* beta FTZ-F1 orphan nuclear receptor provides competence for stage-specific responses to the steroid hormone ecdysone. Mol Cell 3: 143–149.
43. Asahina M, Ishihara T, Jindra M, Kohara Y, Katsura I, et al. (2000) The conserved nuclear receptor Ftz-F1 is required for embryogenesis, moulting and reproduction in *Caenorhabditis elegans*. Genes Cells 5: 711–723.
44. Ding XC, Slack FJ, Grosshans H (2008) The *let-7* microRNA interfaces extensively with the translation machinery to regulate cell differentiation. Cell Cycle 7: 3083–3090.
45. Agawa Y, Sarhan M, Kageyama Y, Akagi K, Takai M, et al. (2007) *Drosophila* Blimp-1 is a transient transcriptional repressor that controls timing of the ecdysone-induced developmental pathway. Mol Cell Biol 27: 8739–8747.
46. Martins G, Calame K (2008) Regulation and functions of Blimp-1 in T and B lymphocytes. Annu Rev Immunol 26: 133–169.
47. Ohinata Y, Payer B, O'Carroll D, Ancelin K, Ono Y, et al. (2005) Blimp1 is a critical determinant of the germ cell lineage in mice. Nature 436: 207–213.
48. Vincent SD, Dunn NR, Sciammas R, Shapiro-Shalef M, Davis MM, et al. (2005) The zinc finger transcriptional repressor Blimp1/Prdm1 is dispensable for early axis formation but is required for specification of primordial germ cells in the mouse. Development 132: 1315–1325.
49. Nie K, Gomez M, Landgraf P, Garcia JF, Liu Y, et al. (2008) MicroRNA-mediated down-regulation of PRDM1/Blimp-1 in Hodgkin/Reed-Sternberg cells: a potential pathogenetic lesion in Hodgkin lymphomas. Am J Pathol 173: 242–252.
50. Matzuk MM (2009) LIN28 lets BLIMP1 take the right course. Dev Cell 17: 160–161.
51. Jones D, Candido EP (2000) The NED-8 conjugating system in *Caenorhabditis elegans* is required for embryogenesis and terminal differentiation of the hypodermis. Dev Biol 226: 152–165.
52. Zhang Y, Grant B, Hirsh D (2001) RME-8, a conserved J-domain protein, is required for endocytosis in *Caenorhabditis elegans*. Mol Biol Cell 12: 2011–2021.
53. Parcej D, Tampe R (2010) ABC proteins in antigen translocation and viral inhibition. Nat Chem Biol 6: 572–580.
54. Lee JI, Dhakal BK, Lee J, Bandyopadhyay J, Jeong SY, et al. (2003) The *Caenorhabditis elegans* homologue of Down syndrome critical region 1, RCN-1, inhibits multiple functions of the phosphatase calcineurin. J Mol Biol 328: 147–156.

55. Goedert M, Baur CP, Ahringer J, Jakes R, Hasegawa M, et al. (1996) PTL-1, a microtubule-associated protein with tau-like repeats from the nematode *Caenorhabditis elegans*. J Cell Sci 109 (Pt 11): 2661–2672.
56. McDermott JB, Aamodt S, Aamodt E (1996) *ptl-1*, a *Caenorhabditis elegans* gene whose products are homologous to the tau microtubule-associated proteins. Biochemistry 35: 9415–9423.
57. Hajduskova M, Jindra M, Herman MA, Asahina M (2009) The nuclear receptor NHR-25 cooperates with the Wnt/beta-catenin asymmetry pathway to control differentiation of the T seam cell in *C. elegans*. J Cell Sci 122: 3051–3060.
58. Hayes GD, Frand AR, Ruvkun G (2006) The *mir-84* and *let-7* paralogous microRNA genes of *Caenorhabditis elegans* direct the cessation of molting via the conserved nuclear hormone receptors NHR-23 and NHR-25. Development 133: 4631–4641.
59. Chen Z, Eastburn DJ, Han M (2004) The *Caenorhabditis elegans* nuclear receptor gene *nhr-25* regulates epidermal cell development. Mol Cell Biol 24: 7345–7358.
60. Slack FJ, Basson M, Liu Z, Ambros V, Horvitz HR, et al. (2000) The *lin-41* RBCC gene acts in the *C. elegans* heterochronic pathway between the *let-7* regulatory RNA and the LIN-29 transcription factor. Mol Cell 5: 659–669.
61. Shi A, Sun L, Banerjee R, Tobin M, Zhang Y, et al. (2009) Regulation of endosomal clathrin and retromer-mediated endosome to Golgi retrograde transport by the J-domain protein RME-8. EMBO J 28: 3290–3302.
62. Fire A, Xu S, Montgomery MK, Kostas SA, Driver SE, et al. (1998) Potent and specific genetic interference by double-stranded RNA in *Caenorhabditis elegans*. Nature 391: 806–811.
63. Simmer F, Tijsterman M, Parrish S, Koushika SP, Nonet ML, et al. (2002) Loss of the putative RNA-directed RNA polymerase RRF-3 makes *C. elegans* hypersensitive to RNAi. Curr Biol 12: 1317–1319.
64. Whitacre J, Bender A (2010) Degeneracy: a design principle for achieving robustness and evolvability. J Theor Biol 263: 143–153.
65. Wagner GP, Pavlicev M, Cheverud JM (2007) The road to modularity. Nat Rev Genet 8: 921–931.
66. Hartwell LH, Hopfield JJ, Leibler S, Murray AW (1999) From molecular to modular cell biology. Nature 402: C47–52.
67. Gunsalus KC, Ge H, Schetter AJ, Goldberg DS, Han JD, et al. (2005) Predictive models of molecular machines involved in *Caenorhabditis elegans* early embryogenesis. Nature 436: 861–865.
68. Peter IS, Davidson EH (2009) Modularity and design principles in the sea urchin embryo gene regulatory network. FEBS Lett 583: 3948–3958.
69. Van Auken K, Weaver DC, Edgar LG, Wood WB (2000) *Caenorhabditis elegans* embryonic axial patterning requires two recently discovered posterior-group Hox genes. Proc Natl Acad Sci U S A 97: 4499–4503.
70. Donaldson JG, Cassel D, Kahn RA, Klausner RD (1992) ADP-ribosylation factor, a small GTP-binding protein, is required for binding of the coatomer protein beta-COP to Golgi membranes. Proc Natl Acad Sci U S A 89: 6408–6412.
71. Li Y, Kelly WG, Logsdon JM, Jr., Schurko AM, Harfe BD, et al. (2004) Functional genomic analysis of the ADP-ribosylation factor family of GTPases: phylogeny among diverse eukaryotes and function in *C. elegans*. FASEB J 18: 1834–1850.
72. Warnock DE, Schmid SL (1996) Dynamin GTPase, a force-generating molecular switch. Bioessays 18: 885–893.
73. Ulrich F, Krieg M, Schotz EM, Link V, Castanon I, et al. (2005) Wnt11 functions in gastrulation by controlling cell cohesion through Rab5c and E-cadherin. Dev Cell 9: 555–564.
74. Hammerschmidt M, Wedlich D (2008) Regulated adhesion as a driving force of gastrulation movements. Development 135: 3625–3641.
75. Fujibayashi A, Taguchi T, Misaki R, Ohtani M, Dohmae N, et al. (2008) Human RME-8 is involved in membrane trafficking through early endosomes. Cell Struct Funct 33: 35–50.
76. Girard M, Poupon V, Blondeau F, McPherson PS (2005) The DnaJ-domain protein RME-8 functions in endosomal trafficking. J Biol Chem 280: 40135–40143.
77. Kay AJ, Hunter CP (2001) CDC-42 regulates PAR protein localization and function to control cellular and embryonic polarity in *C. elegans*. Curr Biol 11: 474–481.
78. Nance J, Priess JR (2002) Cell polarity and gastrulation in *C. elegans*. Development 129: 387–397.
79. Martin AC (2010) Pulsation and stabilization: contractile forces that underlie morphogenesis. Dev Biol 341: 114–125.
80. Bauer R, Lehmann C, Martini J, Eckardt F, Hoch M (2004) Gap junction channel protein innexin 2 is essential for epithelial morphogenesis in the *Drosophila* embryo. Mol Biol Cell 15: 2992–3004.
81. Leithe E, Sirnes S, Omori Y, Rivedal E (2006) Downregulation of gap junctions in cancer cells. Crit Rev Oncog 12: 225–256.
82. Starich T, Sheehan M, Jadrich J, Shaw J (2001) Innexins in *C. elegans*. Cell Commun Adhes 8: 311–314.
83. Kirschner M, Gerhart J (2005) Plausibility of life: great leaps of evolution. New Haven: Yale University Press. 331 p.
84. Gerhart J, Kirschner M (1997) Cells, embryos and evolution: towards a cellular and developmental understanding of phenotypic variation and evolutionary adaptability. Malden, Massachusetts: Blackwell Science. 642 p.
85. Jordan JD, Iyengar R (1998) Modes of interactions between signaling pathways. Biochem Pharmacol 55: 1347–1352.
86. Freeman M (2000) Feedback control of intercellular signalling in development. Nature 408: 313–319.
87. Crews ST, Pearson JC (2009) Transcriptional autoregulation in development. Curr Biol 19: R241–246.
88. Anderson J, Salzer CL, Kumar JP (2006) Regulation of the retinal determination gene dachshund in the embryonic head and developing eye of *Drosophila*. Dev Biol 297: 536–549.
89. Kumar JP (2001) Signalling pathways in *Drosophila* and vertebrate retinal development. Nat Rev Genet 2: 846–857.
90. Mango SE (2009) The molecular basis of organ formation: insights from the *C. elegans* foregut. Annu Rev Cell Dev Biol 25: 597–628.
91. Gaudet J, Mango SE (2002) Regulation of organogenesis by the *Caenorhabditis elegans* FoxA protein PHA-4. Science 295: 821–825.
92. Zhong M, Niu W, Lu ZJ, Sarov M, Murray JI, et al. (2010) Genome-wide identification of binding sites defines distinct functions for *Caenorhabditis elegans* PHA-4/FOXA in development and environmental response. PLoS Genet 6: e1000848. doi:10.1371/journal.pgen.1000848.
93. Conrad M (1990) The geometry of evolution. Biosystems 24: 61–81.
94. Gerhart J, Kirschner M (2007) The theory of facilitated variation. Proc Natl Acad Sci U S A 104 (Suppl 1): 8582–8589.
95. Kirschner M, Gerhart J (1998) Evolvability. Proc Natl Acad Sci U S A 95: 8420–8427.
96. Fitch DH (2000) Evolution of "rhabditidae" and the male tail. J Nematol 32: 235–244.
97. Kiontke K, Fitch DH (2005) The phylogenetic relationships of *Caenorhabditis* and other rhabditids. WormBook. pp 1–11.
98. Brenner S (1974) The genetics of *Caenorhabditis elegans*. Genetics 77: 71–94.
99. Ziel JW, Hagedorn EJ, Audhya A, Sherwood DR (2009) UNC-6 (netrin) orients the invasive membrane of the anchor cell in *C. elegans*. Nat Cell Biol 11: 183–189.
100. Shevchuk NA, Bryksin AV, Nusinovich YA, Cabello FC, Sutherland M, et al. (2004) Construction of long DNA molecules using long PCR-based fusion of several fragments simultaneously. Nucleic Acids Res 32: e19.
101. Shaner NC, Campbell RE, Steinbach PA, Giepmans BN, Palmer AE, et al. (2004) Improved monomeric red, orange and yellow fluorescent proteins derived from Discosoma sp. red fluorescent protein. Nat Biotechnol 22: 1567–1572.